

Nonequilibrium fluctuations in a harmonic trap with annealed stochastic stiffness

Deepak Gupta

E-mail: phydeepak.gupta@gmail.com

Institut für Physik und Astronomie, Technische Universität Berlin, Hardenbergstraße 36, D-10623 Berlin, Germany

Sabine H. L. Klapp

Institut für Physik und Astronomie, Technische Universität Berlin, Hardenbergstraße 36, D-10623 Berlin, Germany

Abstract. We provide a comprehensive analysis of the positional dynamics and average thermodynamics of an overdamped Brownian particle subject to both, harmonic confinement and annealed disorder due to a temporarily fluctuating trap stiffness. We model this stiffness via a stationary Ornstein-Uhlenbeck (OU) process whose correlation time can be tuned from white noise to a quenched limit. We analytically calculate the positional distribution in these limits and provide exact expressions for the n th positional moments at finite correlation times, revealing important insights regarding stationarity. Further, we analyze the average work performed on the particle and the heat dissipated into the environment at all times, illustrating the nonequilibrium character of the system and its relaxation into a steady state. Our analytical results are validated by numerical Langevin simulations.

1. Introduction

It is well established that small-scale systems are typically subject to strong temporal fluctuations [1, 2]. Well-known examples are colloids, polymers, or bio-molecules surrounded by a solvent (the bath) where the typical energy scales of the embedded “system” are comparable to the thermal energy, $k_B T$ (with k_B denoting Boltzmann’s constant and T the temperature) provided by the environment. Assuming a spatially homogeneous environment, and a perfect separation of time scales between system and bath, these thermal fluctuations are often taken account in the spirit of Brownian motion, involving a (coarse-grained) fluctuating force that is Gaussian-distributed, and temporarily uncorrelated [3].

Recently, significant attention has been devoted to systems that are subject to several, not only thermal, types of fluctuations or random disorders. Prominent examples are systems in heterogeneous environments where the bath is not just a

homogeneous background (with spatially constant viscosity and diffusion constant). These play a crucial role in various biological and physical contexts [4–8], such as in intracellular transport [9], protein dynamics on fluctuating membranes [10,11], motion of RNA-protein complexes in live *Escherichia coli* and *Saccharomyces cerevisiae* cells [12], as well as in living yeast cells [13], to name a few.

When investigating disorder effects in theoretical approaches, one has to distinguish between quenched and annealed disorder. Quenched disorder implies that some relevant random parameters do not evolve in time (which implies that the usual ensemble averages have to be supplemented by a disorder average). Exemplary works on the impact of quenched disorder on systems subject to thermal fluctuations concern, e.g., the flocking of active particles [14], phase transitions in random-field Ising model [15] and spin glasses [16], transport in rocking ratchets [17], but also ecological communities [18–20], pattern-forming systems [21], and relaxation processes [22]. In contrast, annealed (or dynamic) disorder means that the parameters characterizing the disorder change in time and are, therefore, in the same time-scales as that of the dynamics of the system. This implies that the usual time-scale separation cannot be performed. Annealed (dynamic) disorder has gained significant attention in models involving fluctuating diffusivity [23–29], consumer-resource dynamics [30], Lotka–Volterra systems [31], and linearly interacting particles’ model [32].

Here, we briefly review the previous research on the annealed disorder. Besides fluctuating diffusion coefficients [23–29], annealed disorder occurs, e.g., when the surrounding medium is near a critical point and exhibits strong density fluctuations, generating a fluctuating viscosity [33,34]. Similarly, stochastic variations in particle mass have motivated models of Brownian particles with short-range attractive interactions and dynamically forming and dissociating clusters [34–36]. Another variant are stochastic modulations of the underlying potential [37–41], and by dragging a probe coupled to fluctuating correlated field [42]. Moreover, stochastic modulation of potentials has also gained interest for implementing finite-time stochastic resetting protocols [43–46] and analyzing the associated thermodynamic costs [47–50]. Along the same line, researchers have discussed the Brownian particle’s position fluctuations by stochastically switching on-off a V -shape potential [51], and a harmonic potential [52]. Ref. [53] discusses the correlations of many particles systems in a harmonic trap with stiffness switching between two values. Further, Refs. [54,55] discusses the shuttling of a quantum particle by stochastically modulating the stiffness and minimum of the trap.

In the present work, we focus on an overdamped Brownian particle in a fluctuating harmonic potential, i.e., a fluctuating trap. Previous works have addressed the positional dynamics in case of a fluctuating trap position (modeled as an Ornstein-Uhlenbeck noise [38,39]). Further, Ref. [37] discusses the stationary state entropy production of a system in fluctuating harmonic potentials. However, a comprehensive understanding of the statistical and thermodynamic properties of a Brownian oscillator with simultaneously or independently fluctuating trap minimum and trap stiffness for a general stochastic fluctuating rule remains limited.

Here, we aim for a detailed analysis of the transient and steady-state dynamics of a harmonically confined Brownian particle in presence of a fluctuating stiffness described as an Ornstein-Uhlenbeck process with persistence time t_p . We also discuss the thermodynamic energy flows. The model may mimic, e.g., a system in a fluctuating potential energy landscape as in occurs in protein folding dynamics [56] where pressure fluctuations change the stiffness of the local harmonic potential (see Fig. 2 in Ref. [56]) without altering the barrier heights. (See also Ref. [37] and references therein for more motivation on this topic.) In our analysis we first obtain the positional distribution in the absence of thermal bath. In the presence of bath, we exactly compute the position distributions in the limit of vanishing ($t_p \rightarrow 0$, white noise limit) and long persistent time ($t_p \rightarrow \infty$, quenched noise limit). For general t_p , we employ the method of subordination [57,58] to exactly compute the n th position's moment. We also discuss the generalization to arbitrary stiffness fluctuations in the limit of weak stiffness noise. Further, to understand the energy cost associated with the stochastic switching of stiffness, we compute exactly the average work performed on the particle and average heat exchanged by the particle with the heat bath at arbitrary times t .

Given that a similar (yet not exactly the same) system has been studied before [59], we briefly summarize the main differences: First, we employ a different white noise's coefficient (motivated from Ref. [30]) in the stiffness-equation (2b); this enables us to explore various noise regimes going from white to quenched disorder in stiffness, when the persistence time becomes large. Second, for this quenched noise limit, we also provide the exact positions' distribution. Third, the positions' fluctuations for general persistent time t_p (2b) are obtained using the method of subordination [57,58] for non-zero initial condition (which is important for the short-time behavior), whereas Ref. [59] uses another method with zero initial condition. Finally, our calculations provide the average heat flow and work done not just in the stationary state [59], but at all times. Overall, our calculations complement the calculations in [59] and provide different technical routes.

The rest of the paper is organized as follows. In the next section 2, we present the model. Section 3 discusses the probability density function of the position of the particle and its associated large deviation function in the absence of thermal noise ($T = 0$). Then, we discuss the position distribution for the case when stiffness behaves as a white noise (i.e., $t_p \rightarrow 0$) in Subsec. 4.1. Subsection 4.2 presents the calculations to obtain the position distribution for stiffness behaving as Gaussian quenched noise (i.e., $t_p \rightarrow \infty$). For finite non-zero t_p , we exactly compute the n th position moment and discuss their stationarity in the long-time limit in Subsec. 4.3. Then, we discuss the average work and average heat flow in Sec. 5. We summarize our main findings in Sec. 6. Appendix A shows the derivation of the Fokker-Planck equation in the white noise limit. Appendix B discusses the solutions of two integrals. Appendix C discusses the detailed calculations to compute the average work.

2. Model

We consider a Brownian particle coupled to a heat bath of temperature T , in a one-dimensional harmonic trap. The trap's net stiffness $[\sigma_0\kappa + \sigma k(t)]$, consists of two contributions, and is stochastic in time. The first one, $\sigma_0\kappa$ is independent of time (where $\kappa > 0$), represent the static stiffness. Moreover, the time-independent parameter σ_0 can be either +1 or -1 or 0 depending on the situation if the static harmonic trap (characterized by κ) is either present [bounded ($\sigma_0 = 1$) or unbounded ($\sigma_0 = -1$)] or absent ($\sigma_0 = 0$). The second contribution involves the stochastic stiffness $\sigma k(t)$, where the time-independent parameter σ controls the strength of the actual stochastic trap's stiffness $k(t)$. We specifically model the stochasticity of the additional stiffness $k(t)$ by a colored noise [see Eq. (1b) below]. [Later in Sec. 4.3, we will discuss a case of general $k(t)$.] Thus, the following Langevin equations of motion describe the full system:

$$\dot{x} = -[\sigma_0 t_k^{-1} + \sigma \gamma^{-1} k(t)]x(t) + \sqrt{2D}\eta(t) , \quad (1a)$$

$$\dot{k} = -\frac{k(t)}{t_p} + \sqrt{A \frac{\theta t_k + 2t_p}{t_p^2}} \xi(t) , \quad (1b)$$

where the dot denotes a time derivative, and $t_k \equiv \gamma/\kappa$ is the harmonic trap's relaxation time in the absence of $k(t)$ with friction constant γ . Further, $D = k_B T/\gamma$ is the diffusion constant, and $\eta(t)$ and $\xi(t)$, respectively, are Gaussian white noises with zero mean and delta correlation in time, i.e., $\langle \eta(t)\eta(t') \rangle = \delta(t-t')$ and $\langle \xi(t)\xi(t') \rangle = \delta(t-t')$. Also, $\eta(t)$ and $\xi(t)$ are independent of each other, i.e., $\langle \eta(t)\xi(t') \rangle = 0$ for all t, t' . Here, the brackets $\langle \dots \rangle$ indicate the ensemble average over the noise realizations.

In Eq. (1b), t_p is the persistence time. The prefactor $\sqrt{A(\theta t_k + 2t_p)/t_p^2}$ of the noise $\xi(t)$ is motivated from Ref. [30] where it was introduced to understand the role of environmental fluctuations on the species abundance distribution in an ecological community. Later in this section, we will discuss the significance of this prefactor in the present context. We also note that the prefactor is different from that chose in Ref. [59].

To make the equations (1) dimensionless, we rescale the particle's position, time, and spring constant, and the parameter A using the length $\sqrt{Dt_k}$, the relaxation time t_k , and the static spring constant κ , respectively, $x/\sqrt{Dt_k} \rightarrow x$, $t/t_k \rightarrow t$, $t_p/t_k \rightarrow t_p$, $k/\kappa \rightarrow k$, $A/\kappa^2 \rightarrow A$. The Langevin equations (1) then read

$$\dot{x} = -[\sigma_0 + \sigma k(t)]x(t) + \sqrt{2}\eta(t) , \quad (2a)$$

$$\dot{k} = -\frac{k(t)}{t_p} + \sqrt{A \frac{\theta + 2t_p}{t_p^2}} \xi(t) . \quad (2b)$$

The probability density function of x depends on the fluctuations of $\eta(t)$ and $k(t)$. Since the distribution of $\xi(t)$ is Gaussian, the probability density function of stiffness $k(t)$ at each time t is also Gaussian, with mean μ_k and variance Σ_k^2

$$\mu_k \equiv \langle k(t) \rangle = k_0 e^{-t/t_p} , \quad (3a)$$

$$\Sigma_k^2 \equiv \langle \delta k(t)^2 \rangle = A \frac{\theta + 2t_p}{2t_p} (1 - e^{-2t/t_p}) , \quad (3b)$$

for fixed initial condition $k_0 \equiv k(0)$. Here, $\delta k(t) \equiv k(t) - \langle k(t) \rangle$ is the deviation of k from its mean value. Further, it is straightforward to compute the two-point correlation function as

$$\langle \delta k(t) \delta k(t') \rangle = A \frac{\theta + 2t_p}{2t_p} [e^{-|t-t'|/t_p} - e^{-(t+t')/t_p}] . \quad (4)$$

In the long-time limit (i.e., $t \gg t_p$), the distribution of $k(t)$ becomes stationary, and its explicit expression is given by

$$p_{ss}(k) = \frac{1}{\sqrt{2\pi\Sigma_{k,ss}^2}} \exp \left[-\frac{(k - \mu_{k,ss})^2}{2\Sigma_{k,ss}^2} \right] , \quad (5)$$

with mean $\mu_{k,ss} = 0$, and variance $\Sigma_{k,ss}^2 = A \frac{\theta + 2t_p}{2t_p}$. Further, the two-point correlation (4) becomes

$$\langle \delta k(t) \delta k(t') \rangle_{ss} = A \frac{\theta + 2t_p}{2t_p} e^{-|t-t'|/t_p} . \quad (6)$$

Henceforth, we drop δ from δk as the mean of k is zero in the stationary state. In the limit cases of zero and diverging t_p , the two point correlation function behaves as

$$\langle k(t) k(t') \rangle_{ss} = \begin{cases} A\theta\delta(t-t') & t_p \rightarrow 0 \\ A & t_p \rightarrow \infty \end{cases} . \quad (7)$$

Equation (7) reveals that the choice of the prefactor in front of $\xi(t)$ (2b) (considered previously in Ref. [30]) allows us explore different types of $k(t)$. These are Gaussian white noise ($t_p \rightarrow 0$), Gaussian quenched noise ($t_p \rightarrow \infty$), and colored noise for finite non-zero t_p . The Gaussian quenched noise ($t_p \rightarrow \infty$) implies that the stiffness's value $k(t)$ is fixed for all time (7), but is drawn initially from a Gaussian distribution with zero mean and A variance. Thus, the stochasticity of the additional noise $k(t)$ arises from its initial condition.

In contrast to the stiffness's distribution $p(k, t)$, the probability density function $P(x, t|x_0)$ is not expected to be Gaussian, for the particle starting from x_0 . In the following, we aim to compute the full positions' fluctuations of the particle with initial condition x_0 and k_0 , where the latter are drawn from the stationary distribution (5).

3. Absence of heat bath: $T = 0$

In this section, we focus on a harmonic oscillator in the absence of external heat bath, i.e., $D = 0$. (Notice that we can still use the Dt_k as a length scale to rescale the position, where D corresponds to an equivalent thermal system.) Therefore, the system

is described by the Langevin equations (2) in the absence of $\eta(t)$. Substituting $x = e^y$ (for $x \geq 0$) in Eq. (1a), we have

$$\frac{dy(t)}{dt} = -[\sigma_0 + \sigma k(t)] , \quad (8)$$

where $y \in (-\infty, \infty)$.

In the following, we compute the distribution of y at time t given the stationary state fluctuations of k are described by Eq. (2b). Since $y(t)$ is linear in $k(t)$ (Gaussian distributed noise), the distribution of $y(t)$ will also be Gaussian. Therefore, we only require its mean and variance to characterize its fluctuations. To this end, we solve Eq. (8), yielding

$$y(t) = y(0) - \sigma_0 t - \sigma \int_0^t dt' k(t') , \quad (9)$$

for the initial condition $y(0) = \ln x_0$. Averaging over trajectories of $k(t)$ given that its initial condition k_0 is drawn from the stationary distribution $p_{ss}(k_0)$ (5), we obtain the mean

$$\mu_y \equiv \langle y(t) \rangle = y(0) - \sigma_0 t . \quad (10)$$

The variance of y can be computed via

$$\begin{aligned} \sigma_y^2 \equiv \langle \delta y(t)^2 \rangle &= \sigma^2 \int_0^t dt_1 \int_0^t dt_2 \langle k(t_1) k(t_2) \rangle_{ss} , \\ &= -\sigma^2 H_1(t) . \end{aligned} \quad (11)$$

where we substituted the two-point correlation, $\langle k(t_1) k(t_2) \rangle_{ss}$, from Eq. (6). Further, $\delta y(t) \equiv y(t) - \langle y(t) \rangle$ is the deviation of y from its mean value, and we defined

$$H_1(t) \equiv At_p(\theta + 2t_p)(1 - t/t_p - e^{-t/t_p}) . \quad (12)$$

Given the y -distribution, $\pi(y, t|y(0))$, we obtain the position distribution while using the Jacobian of transformation of variables. It turns out that the positions' fluctuations are log-normal distributed, that is,

$$P(x, t|x_0) = \pi(y, t|y(0)) \left| \frac{dy}{dx} \right| = \frac{\exp \left[-\frac{(\ln x - \mu_y)^2}{2\sigma_y^2} \right]}{x \sqrt{2\pi\sigma_y^2}} , \quad (13)$$

for $x \geq 0$. For $x \leq 0$, the above expression still holds by simply replacing $x \rightarrow |x|$. Therefore, the motion of the particle is restricted to either sides of the origin if the particle starts from $x_0 \neq 0$. This behavior of the system can be intuitively understood as follows. In the absence of thermal noise [see Eq. (2)], the position of the particle evolves as $\dot{x}(t) = -[\sigma_0 + \sigma k(t)]x(t)$. Therefore, a large positive value of $k(t)$ will bring the particle to origin, whereas a large negative value pushes the particle to either $x = +\infty$

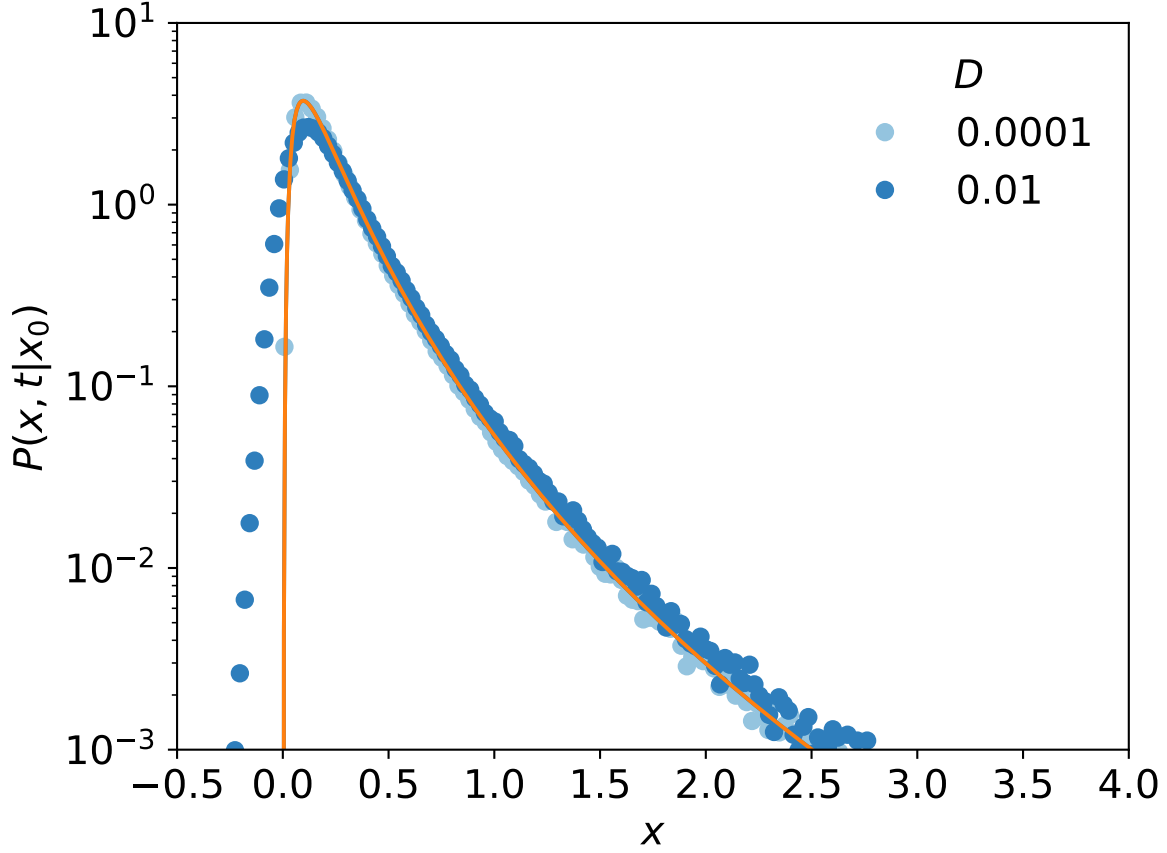


Figure 1. Comparison of the analytical probability density function for $D = 0$ (13) and the numerically simulated distribution using Eq. (1) for $D = 10^{-4}, 10^{-2}$. Other fixed parameters are $x_0 = 0.5$, $t_p = 1.0$, $A = 2$, $\theta = 1.5$, $\sigma = 0.5$, and $t = 1$. Solid line: Analytical result. Symbols: Numerical Langevin simulation (number of realizations: 10^6).

or $x = -\infty$, depending on whether the particle started from $x_0 > 0$ or $x_0 < 0$, respectively. Thus, the particle (for $D = 0$) is unable to cross the origin if it starts from $x_0 \neq 0$.

Figure 1 shows the comparison of analytical expression for the probability density (13) with numerical Langevin simulation performed for different thermal noise amplitude D . As expected, for sufficient smaller D , the numerical Langevin simulation result ($D \neq 0$) agrees with the analytical result for $D = 0$. As soon as D becomes larger the distribution departs from the log-normal distribution.

We further note that we can rewrite $P(x, t|x_0)$ (13) for $\sigma_0 \neq 0$ as

$$P(z, t|z_0) = \frac{|\sigma_0|t}{\sqrt{2\pi\sigma_y^2}} \exp\left[-\frac{t^2\sigma_0^2(z - z_0 + 1)^2}{2\sigma_y^2}\right], \quad (14)$$

where we defined $z \equiv \frac{\ln|x|}{\sigma_0 t}$ and $z_0 \equiv \frac{\ln|x_0|}{\sigma_0 t}$. In the long time limit $t \gg \sigma_0^{-1} \ln|x_0|$ (i.e., $z_0 \ll 1$), the probability density function (14) assumes the large-deviation form [60]

$$P(z, t) \approx e^{-tI(z)} \quad (15)$$

with the large deviation function (LDF)

$$I(z) = \frac{\sigma_0^2(z+1)^2}{2\sigma^2 A(\theta + 2t_p)} . \quad (16)$$

Similarly, for $\sigma_0 = 0$, $P(x, t|x_0)$ (13) can be rewritten as

$$P(z, t|z_0) = \frac{t}{\sqrt{2\pi\sigma_y^2}} \exp\left[-t^2 \frac{(z - z_0)^2}{2\sigma_y^2}\right] , \quad (17)$$

where we defined $z \equiv \frac{\ln|x|}{t}$ and $z_0 \equiv \frac{\ln|x_0|}{t}$. In the long time limit $t \gg \ln|x_0|$ (i.e., $z_0 \ll 1$), we then obtain the large deviation form

$$P(z, t) \approx e^{-tI(z)} \quad (18)$$

with the LDF

$$I(z) = \frac{z^2}{2\sigma^2 A(\theta + 2t_p)} . \quad (19)$$

The LDFs (16) and (19), respectively, describe the asymptotic form of the probability density functions (PDFs) (14) and (17) in the long time limit: The LDF essentially describes that the deviation from the typical fluctuations (around the minimum of the LDF) are exponentially unlikely in the long-time limit [60].

4. Presence of heat bath: $T \neq 0$

We now analyze the positions' fluctuations when $D \neq 0$. We first investigate two particular limits of the persistence time t_p entering in Eq. (2b): These are, 1) $t_p \rightarrow 0$ (Gaussian white noise) and 2) $t_p \rightarrow \infty$ (quenched noise). We then consider the case of general t_p . We here recall that the consideration of the different limits of t_p is possible due to our choice of the prefactor in front of $\xi(t)$ [Eq.(2b)].

4.1. White noise: $t_p \rightarrow 0$

The limit $t_p \rightarrow 0$ leads to the white noise limiting behavior [see first line of Eq. (7)] of the full system, i.e., $k(t)$ is replaced by $\sqrt{A\theta}\xi(t)$ in Eq. (2a). Given this, we herein compute the probability density function of this system.

The Fokker-Planck equation (following Stratonovich's rule) corresponding to this system can be obtained as (see Appendix A for its detailed derivation)

$$\frac{\partial P(x, t|x_0)}{\partial t} = \frac{\partial}{\partial x} \left[(\sigma_0 - a^2/2)x P(x, t|x_0) \right] + \frac{\partial^2}{\partial x^2} \left[(1 + a^2 x^2/2) P(x, t|x_0) \right] , \quad (20)$$

for the initial condition $P(x, t|x_0) = \delta(x - x_0)$ and $a \equiv \sigma\sqrt{A\theta}$. In the above equation (20), on the right-hand side, the terms proportional to a^2 are due to the stochastic white-noise stiffness.

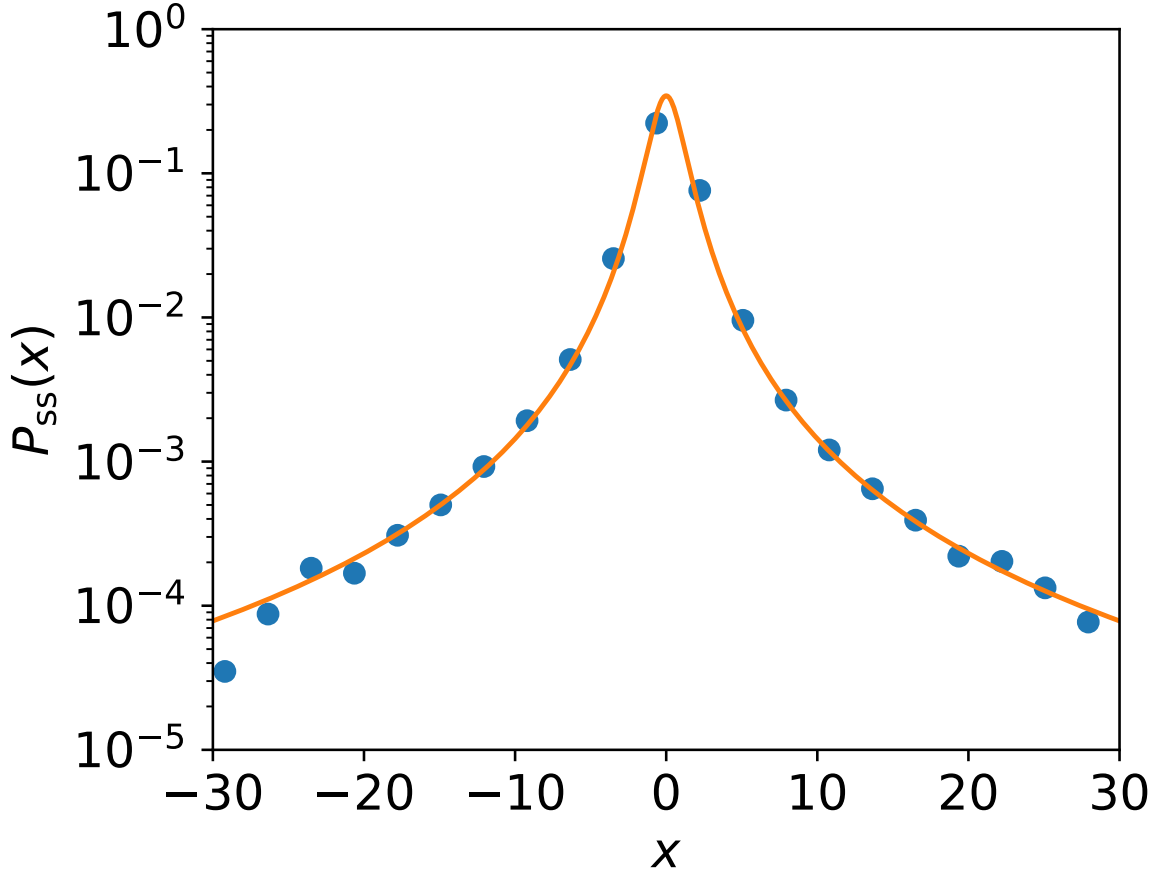


Figure 2. Comparison of analytical stationary state and numerical Langevin simulation data obtained at $t = 50$ in the white noise limiting case ($t_p \rightarrow 0$). Other fixed parameters are $A = 1$, $\theta = 1.2$, $\sigma_0 = 1$, and $\sigma = 1$. $t = 50$. Solid line: Analytical result (21). Symbols: Numerical Langevin simulation.

The stationary state of the system can be obtained by setting the left hand side of Eq. (20) equal to zero. It turns out that the stationary state probability density function is normalized only if $\sigma_0 > 0$, i.e., the system has a stationary state only if the underlying static harmonic potential is bounded (i.e., $\sigma_0 > 0$). This stationary distribution is given by

$$P_{ss}(x) = \frac{a}{\sqrt{\pi}} \frac{2^{\frac{\sigma_0}{a^2}} \Gamma\left(\frac{1}{2} + \frac{\sigma_0}{a^2}\right)}{\Gamma\left(\frac{\sigma_0}{a^2}\right)} \frac{1}{(2 + a^2 x^2)^{\frac{2\sigma_0 + a^2}{2a^2}}} . \quad (21)$$

Thus, the positions' fluctuations in the stationary state have a power-law distribution and its tails decay as $|x|^{-(1+2\sigma_0/a^2)}$ as $|x| \rightarrow \infty$. Figure (2) shows the agreement of the analytical result (21) with the numerical Langevin simulation data at $t = 50$. Further, in the limit of vanishing stiffness' noise parameter (i.e., $a \rightarrow 0$), the stationary distribution (21) becomes a Gibbs' distribution

$$P_{ss}(x) \approx \mathcal{N}[1 - a^2(\sigma_0/a^2 + 1/2)x^2/2] \rightarrow \mathcal{N}e^{-\sigma_0 x^2/2} , \quad (22)$$

as expected, for the normalization constant \mathcal{N} .

Using this stationary state (21), we compute the n th position moment and find that

$$\langle x^n \rangle_{\text{ss}} = \frac{2^{\frac{n}{2}-1} [(-1)^n + 1] a^{-n} \Gamma\left(\frac{n+1}{2}\right) \Gamma\left(\frac{\sigma_0}{a^2} - \frac{n}{2}\right)}{\sqrt{\pi} \Gamma\left(\frac{\sigma_0}{a^2}\right)}. \quad (23)$$

Equation (23) shows that the moments exist for $a^2 < 2\sigma_0/n$.

4.2. Quenched noise: $t_p \rightarrow \infty$

In the limit of long-persistence time ($t_p \rightarrow \infty$), the stochastic stiffness $k(t)$ is effectively constant in time and behaves as a quenched Gaussian random variable [see the discussion below Eq. (7), and Eq. (27) below] with zero mean and A variance [see Eqs. (2b), (6)]. [Notice that the quenched disorder appears in our model due to the prefactor (different compared to Ref. [59]) in front of $\xi(t)$ (1b).] Therefore, for each given initial value of k [drawn from the stationary distribution $p_{\text{ss}}(k) \propto e^{-k^2/(2A)}$], the probability density function of the particle's position is a Gaussian distribution

$$p(x, t; k|x_0) = \frac{1}{\sqrt{2\pi\Sigma^2(t; k)}} \exp\left[-\frac{[x - \mu(t; k)]^2}{2\Sigma^2(t; k)}\right], \quad (24)$$

where the mean and variance, respectively, follows as

$$\mu(t; k) = x_0 e^{-(\sigma_0 + \sigma k)t}, \quad (25)$$

$$\Sigma^2(t; k) = \frac{1 - e^{-2(\sigma_0 + \sigma k)t}}{\sigma_0 + \sigma k}. \quad (26)$$

We are now in the position to obtain the distribution of x at time t by averaging $p(x, t; k|x_0)$ over the distribution of k -values, yielding

$$P(x, t|x_0) = \int_{-\infty}^{+\infty} dk \, p_{\text{ss}}(k) \, p(x, t; k|x_0) \quad (27)$$

$$= \frac{1}{2\pi\sigma\sqrt{At}} \int_0^{+\infty} \frac{dy}{y} \sqrt{\frac{\ln y}{t(y^2 - 1)}} e^{-\frac{(\ln y + \sigma_0 t)^2}{2A\sigma^2 t^2}} e^{-\frac{\ln y}{t} \frac{(x - x_0 y)^2}{2(y^2 - 1)}}. \quad (28)$$

To reach Eq. (28) from Eq. (27), we made a change of variables such that $k = -(\sigma_0 t + \ln y)/(\sigma t)$. Notice that, unlike the case of a harmonic oscillator with a fixed (non-random) stiffness—where the distribution remains Gaussian at all times—here, due to the quenched stochastic stiffness, the resulting distribution is not necessarily Gaussian (see dashed lines in Fig. 3).

It is readily possible to evaluate the integral in Eq. (28) numerically. Still, it is interesting to find an approximation of the above integral (28) when the external noise

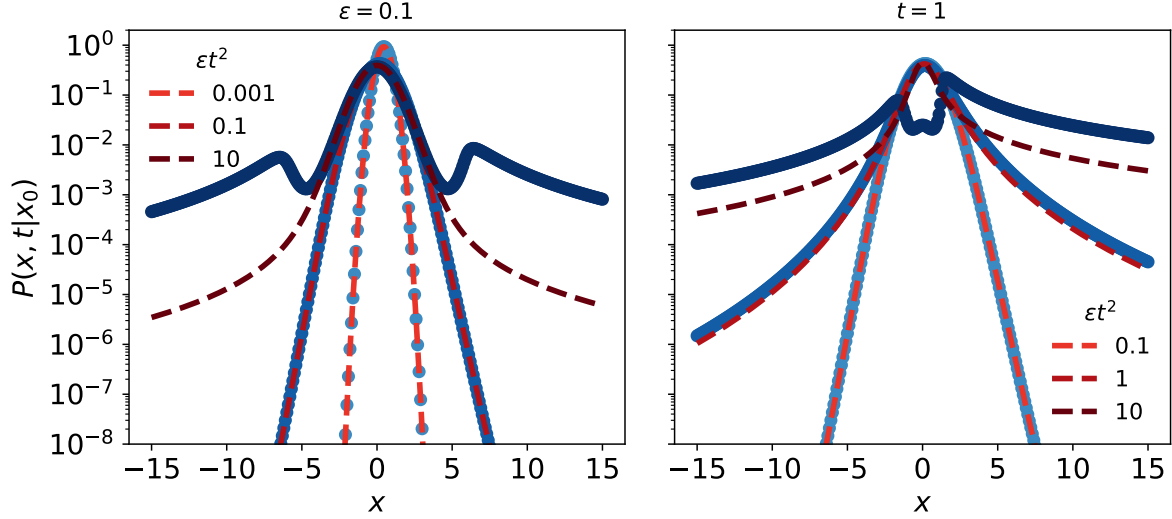


Figure 3. Comparison of saddle-point (blue symbol) approximated distribution (31) with the exact (red dashed line) distribution (29) in the quenched noise case ($t_p \rightarrow \infty$). We fixed $\sigma_0 = 1$ and the initial position $x_0 = 0.5$. Color intensity increases with increasing ϵt^2 .

strength, $\sigma^2 A$, is vanishingly small. This can be done by using the saddle-point method. To this end, we rewrite the above integral (28) as

$$P(x, t|x_0) = \frac{1}{2\pi\sqrt{\epsilon t}} \int_0^\infty dy \exp\left[-\frac{1}{2\epsilon t^2} f(y; x, t, x_0, \epsilon)\right] \quad (29)$$

where we defined $\epsilon \equiv \sigma^2 A$, and

$$f(y; x, t, x_0, \epsilon) \equiv \epsilon t^2 \ln\left(\frac{ty^2(y^2 - 1)}{\ln y}\right) + \epsilon t \ln y \frac{(x - x_0 y)^2}{(y^2 - 1)} + (\sigma_0 t + \ln y)^2. \quad (30)$$

Considering ϵt^2 as a small parameter (i.e., $\epsilon t^2 \ll 1$), we can approximate the above integral using the saddle-point method. This gives

$$P(x, t|x_0) \approx \frac{\exp\left(-\frac{f(y^*)}{2\epsilon t^2}\right)}{\sqrt{4\pi f''(y^*)}} \left[1 + \text{Erf}\left(y^*(x) \sqrt{\frac{f''(y^*)}{4\epsilon t^2}}\right)\right], \quad (31)$$

where $y^* \equiv y^*(x, t, x_0, \epsilon)$ is the saddle-point obtained by solving

$$\partial_y f(y; x, t, x_0, \epsilon)|_{y=y^*} = 0. \quad (32)$$

For convenience, in Eq. (31) we used the notation $f(y^*) \equiv f(y^*; x, t, x_0, \epsilon)$ and $f''(y) \equiv \partial_y^2 f(y; x, t, x_0, \epsilon)|_{y=y^*}$.

Figure 3 shows the comparison of the saddle-point result (31) with the exact distribution (29) for different values of ϵt^2 and fixed $\sigma_0 = 1$ (similar findings occur for $\sigma_0 \leq 0$). The data shows that the saddle-point approximation becomes increasingly

better as ϵt^2 decreases. Finally, we here remark that for $\sigma_0 > 0$ and in the long-time limit, the system will approach a stationary state in the limit $\epsilon \rightarrow 0$. For other cases of σ_0 , the system does not have a stationary state even in this limit ($\epsilon \rightarrow 0$) due to the non-positive value of stiffness k , as expected.

4.3. General t_p

In this section, we treat the full model (2a) with $D \neq 0$. To compute the the probability density function of particle's position, we solve the Fokker-Planck equation for each realization of $k(t)$, given as

$$\frac{\partial p(x, t; k(t))}{\partial t} = \frac{\partial}{\partial x} [(\sigma_0 + \sigma k(t)) x p(x, t; k(t))] + \frac{\partial^2 p(x, t; k(t))}{\partial x^2} , \quad (33)$$

for initial condition $p(x, 0; k_0) = \delta(x - x_0)$ for all $k_0 \equiv k(0)$. Notice here that k_0 are distributed according to the stationary distribution $p_{ss}(k_0)$ (5). Therefore, once $p(x, t; k(t))$ is known, we perform the average

$$P(x, t | x_0) = \langle p(x, t; k(t)) \rangle_{\{k(t)\}} , \quad (34)$$

over the ensemble of trajectories of $k(t)$ emanating from k_0 , where k_0 is drawn from $p_{ss}(k_0)$ (5)

To solve the Fokker-Planck equation (33) for a given realization of $k(t)$, we use the method of subordination [57, 58]. This implies the substitution

$$p(x, t; k(t)) = f(t) Q(z(x, t), \tau(t)) , \quad (35)$$

where

$$f(t) \equiv e^{\sigma_0 t + \sigma \int_0^t ds k(s)} , \quad (36a)$$

$$z(x, t) \equiv x f(t) , \quad (36b)$$

$$\tau(t) \equiv \int_0^t ds f^2(s) , \quad (36c)$$

for the initial condition $z(x, 0) = x_0$, in Eq. (33). With this substitution, the Fokker-Planck equation (33) translates into a diffusion equation

$$\partial_\tau Q(z, \tau) = \partial_z^2 Q(z, \tau) , \quad (37)$$

with the stochastic time τ (36c). Equation (37) is supplemented by the initial condition $Q(z, 0) = \delta(z - x_0)$. For convenience, we henceforth drop the explicit dependence of x and t from z and τ .

The solution of Eq. (37) can be obtained using the Fourier-Transform

$$Q(z, \tau) = \frac{1}{2\pi} \int_{-\infty}^{+\infty} dp e^{-p^2 \tau} e^{ip(z-x_0)} = \frac{1}{2\pi} \int_{-\infty}^{+\infty} dp e^{-ipx_0} e^{ipx f(t)} e^{-p^2 \tau(t)} , \quad (38)$$

where p is the conjugate variable with respect to z , and we have substituted z from Eq. (36b).

Substituting (38) for $Q(z, \tau)$ into Eq. (35), and writing the annealed average (34) over the ensemble of trajectories of $k(t)$, we have

$$P(x, t|x_0) = \left\langle \int_{-\infty}^{+\infty} dp f(t) \frac{e^{-ipx_0}}{2\pi} e^{-p^2 \tau(t)} e^{ipx f(t)} \right\rangle_{\{k(t)\}}. \quad (39)$$

Henceforth, for notational simplicity, we drop the subscript $\{k(t)\}$ from the angled brackets. Due to the complicated structure of $f(t)$ (36a) as well as $\tau(t)$ (36c) entering in the exponents in Eq. (39), the computation of the ensemble average (39) to obtain the probability density function is not straightforward. Nonetheless, Eq. (39) provides the basis to compute the n th moment of the position of the particle. To this end, we multiply x^n on both sides of Eq. (39) and integrate from $x = -\infty$ to $x = +\infty$. This gives

$$\langle x^n \rangle = \sum_{q=0, q \in \mathbb{Z}^+}^{n/2} \binom{n}{2q} \frac{4^q}{\sqrt{\pi}} \Gamma\left(\frac{1+2q}{2}\right) x_0^{n-2q} \langle f^{-n} \tau^q \rangle, \quad (40)$$

where, for convenience, we have dropped the explicit dependence of t from $f(t)$ and $\tau(t)$. Here, we remark that our results in this section generalizes that of Ref. [59], by considering the non-zero initial position ($x_0 \neq 0$). Moreover, the method used in this paper (method of substitution) is different than that of used in Ref. [59].

For $n = 0$, both sides give unity, as expected. To compute the n th moment, we have to evaluate the right-most term, i.e., the average. In the following, we discuss the method to compute this quantity.

We start from the explicit expression for the average,

$$\begin{aligned} \langle f^{-n} \tau^q \rangle &= \left\langle e^{-n\sigma_0 t} e^{-n\sigma \int_0^t ds k(s)} \prod_{j=1}^q \int_0^t ds_j e^{2\sigma_0 s_j} e^{2\sigma \int_0^{s_j} da_j k(a_j)} \right\rangle \\ &= e^{-n\sigma_0 t} \left(\prod_{j=1}^q \int_0^t ds_j \right) e^{2\sigma_0 \sum_{\ell=1}^q s_\ell} \left\langle e^{-\sigma \left[n \int_0^t ds k(s) - 2 \sum_{m=1}^q \int_0^{s_m} da_m k(a_m) \right]} \right\rangle. \end{aligned} \quad (41)$$

We now use the fact that for a random variable Y , the cumulant generating function is $\ln \langle e^{-\sigma Y} \rangle = \sum_{m=1}^{\infty} \frac{(-\sigma)^m}{m!} \langle\langle Y^m \rangle\rangle$, where the double angled brackets indicates the cumulant. Thus,

$$\begin{aligned} \langle f^{-n} \tau^q \rangle &= e^{-n\sigma_0 t} \left(\prod_{j=1}^q \int_0^t ds_j \right) e^{2\sigma_0 \sum_{\ell=1}^q s_\ell} \times \\ &\times \exp \left[\sum_{m=1}^{\infty} \frac{(-\sigma)^m}{m!} \left\langle\left\langle \left[n \int_0^t ds k(s) - 2 \sum_{m=1}^q \int_0^{s_m} da_m k(a_m) \right]^m \right\rangle\right\rangle \right]. \end{aligned} \quad (42)$$

We emphasize that the above expression is exact and does not depend on the underlying dynamics of $k(t)$.

Since the term insider the square bracket is Gaussian random variable [as in our case (2b)], the cumulants of order larger than 2 (i.e., $m > 2$) are zero. Further, the term

corresponding to $m = 1$ is also zero as the first cumulant or the mean of $k(t)$ is zero. Equation (42) thus reduces to

$$\begin{aligned} \langle f^{-n} \tau^q \rangle &= e^{-n\sigma_0 t} \left(\prod_{j=1}^q \int_0^t ds_j \right) e^{2\sigma_0 \sum_{\ell=1}^q s_\ell} \times \\ &\times \exp \left[\frac{\sigma^2}{2} \left\langle \left\langle \left[n \int_0^t ds k(s) - 2 \sum_{m=1}^q \int_0^{s_m} da_m k(a_m) \right]^2 \right\rangle \right\rangle \right]. \end{aligned} \quad (43)$$

We here remark that in some cases, the dynamics of $k(t)$ may be governed by a complex stochastic process that reaches a stationary state at long times. In such situations, calculating fluctuations in the position (position's moments) is not straightforward. However, when the stochastic stiffness is weak (i.e., $\sigma \rightarrow 0$), we can still compute the moments of the position by using the average $\langle f^{-n} \tau^q \rangle$ from Eq. (43) in Eq. (40). This average captures the leading contributions of order σ^2 , assuming that higher-order cumulants $\langle\langle k^n(t) \rangle\rangle$ remain finite for $n > 2$. Additionally, if the stationary process $k(t)$ has a nonzero mean $\langle k(t) \rangle_{\text{ss}}$, we can shift it to zero by redefining σ_0 as $\sigma_0 + \sigma \langle k(t) \rangle_{\text{ss}}$.

Coming back to Eq. (43), inside the exponential, we expand the square bracket and use the expression (6) for $\langle\langle k(t)k(s) \rangle\rangle$ since $k(t) = 0$. Performing the integrals, we obtain

$$\langle f^{-n} \tau^q \rangle = e^{-n\sigma_0 t} \left(\prod_{j=1}^q \int_0^t ds_j \right) e^{2\sigma_0 \sum_{\ell=1}^q s_\ell} e^{-\frac{\sigma^2}{2} [n^2 H_1(t) + 4 \sum_{m_1=1}^q \sum_{m_2=1}^q H_2(s_{m_1}, s_{m_2}) - 4n \sum_{m=1}^q H_2(t, s_m)]}, \quad (44)$$

where we defined

$$H_2(s_1, s_2) \equiv \frac{1}{2} A t_p (\theta + 2t_p) \left[1 - 2 \frac{\min(s_1, s_2)}{t_p} + e^{-\frac{|s_1 - s_2|}{t_p}} - e^{-\frac{s_1}{t_p}} - e^{-\frac{s_2}{t_p}} \right], \quad (45)$$

and $H_1(t) = H_2(t, t)$ [$H_1(t)$ is given in Eq. (12)]. Finally, substituting Eq. (44) into the right-hand side of Eq. (40), we obtain the expression for all moments.

In the following, we obtain the first four positional moments using Eq. (40). For $n = 1$, we get

$$\langle x \rangle = x_0 \langle f^{-1}(t) \rangle = x_0 e^{-\sigma_0 t} e^{-\sigma^2 H_1(t)/2}. \quad (46)$$

In the long-time limit, $H_1(t)$ behaves as $H_1(t) \approx -A(\theta + 2t_p)t$. Therefore, the first moment reach a stationary value $\langle x \rangle_{t \rightarrow \infty} = 0$, when the parameter combination is such that $A\sigma^2(\theta + 2t_p) \leq 2\sigma_0$. Thus, the mean position always diverges for the unbounded system $\sigma_0 \leq 0$ for non-zero initial condition $x_0 \neq 0$.

Let us now compute the second moment ($n = 2$) using Eq. (40). We find

$$\langle x^2 \rangle = x_0^2 \langle f^{-2}(t) \rangle + 2 \langle f^{-2}(t) \tau(t) \rangle = x_0^2 e^{-2\sigma_0 t} e^{-2\sigma^2 H_1(t)} + 2 \underbrace{\int_0^t ds e^{-2\sigma_0 s} e^{-2\sigma^2 H_1(s)}}_{\mathcal{I}_1} \quad (47)$$

$$= x_0^2 e^{-2\sigma_0 t} e^{-2\sigma^2 H_1(t)} + 2t_p e^{-\alpha} (-\alpha)^{-b} \left[\Gamma\left(b, -e^{-\frac{t}{t_p}} \alpha\right) - \Gamma(b, -\alpha) \right], \text{ for } t_p > 0 \quad (48)$$

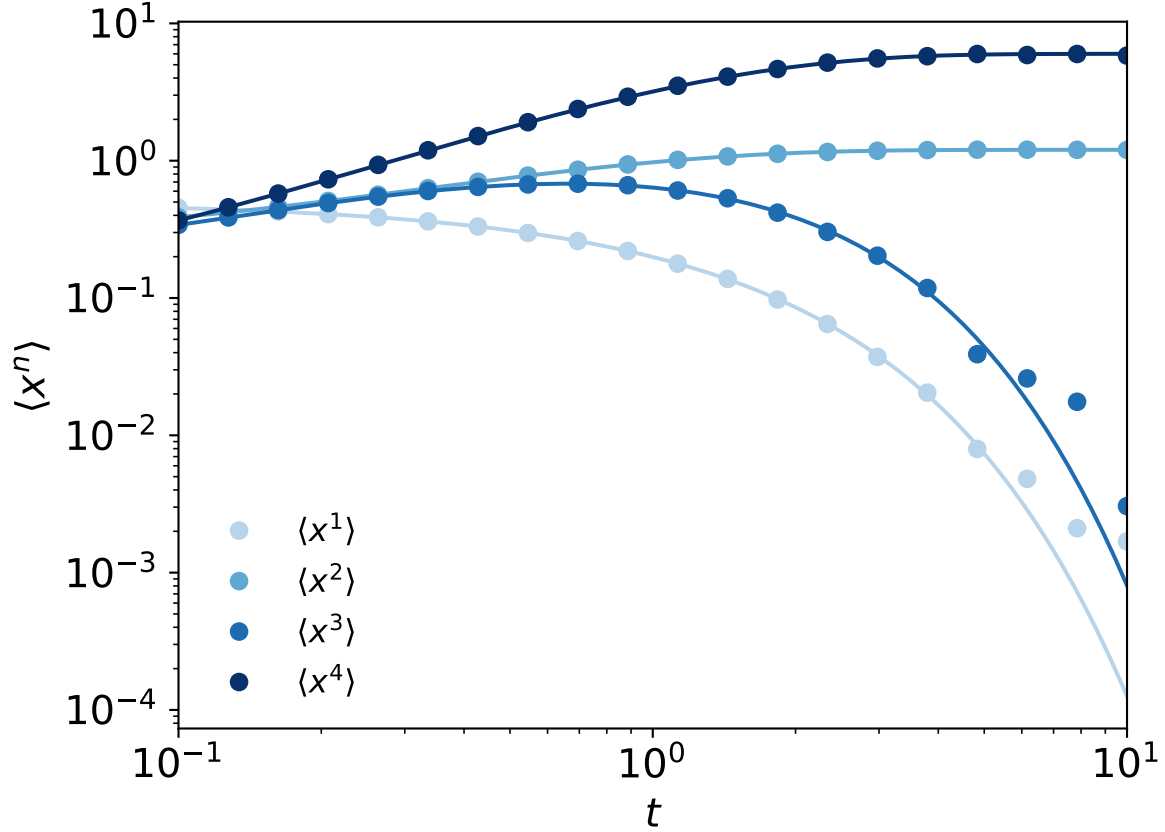


Figure 4. Comparison of analytical results for the moments with the numerical simulations. We take the parameters $x_0 = 0.5$, $\sigma = 0.65$, $t_p = 0.8$, $\theta = 0.6$, $A = 0.4$ such that $A\sigma^2(\theta + 2t_p) = 0.3718$. $dt = 10^{-4}$. Number of realizations 10^6 . Solid lines: Analytical results (46), (48), (51), and (52). Circles: Numerical Langevin simulations.

where $\Gamma(b, y) = \int_y^\infty x^{b-1} e^{-x}$ is the incomplete gamma function, and we defined $\alpha \equiv 2\sigma^2 A t_p (\theta + 2t_p)$ and $b \equiv 2\sigma_0 t_p - \alpha$ (see Appendix B.1 for the computation of \mathcal{I}_1). In the long-time limit, the second moment reaches a stationary value

$$\langle x^2 \rangle_{t \rightarrow \infty} = 2t_p e^{-\alpha} (-\alpha)^{-b} [\Gamma(b) - \Gamma(b, -\alpha)] , \quad (49)$$

when $b > 0$. Therefore, the second moment reaches a stationary value if $A\sigma^2(\theta + 2t_p) < \sigma_0$.

The third moment ($n = 3$) follows as

$$\begin{aligned} \langle x^3 \rangle &= x_0^3 \langle f^{-3} \rangle + 6x_0 \langle f^{-3} \tau^1 \rangle \\ &= x_0^3 e^{-3\sigma_0 t} e^{-9\sigma^2/2 H_1(t)} + 6x_0 e^{-3\sigma_0 t} e^{-9\sigma^2/2 H_1(t)} \underbrace{\int_0^t ds e^{2\sigma_0 s} e^{-2\sigma^2 [H_2(s, s) - 3H_2(t, s)]}}_{\mathcal{I}_2} \end{aligned} \quad (50)$$

$$\begin{aligned} &= x_0^3 e^{-3\sigma_0 t} e^{-9\sigma^2/2 H_1(t)} + 6x_0 t_p e^{\alpha/2} e^{-\frac{3\alpha}{2} e^{-t/t_p}} e^{-3\sigma_0 t} e^{-9\sigma^2/2 H_1(t)} \times \\ &\times \sum_{m=0}^{\infty} \frac{(3\alpha/2)^m e^{-mt/t_p}}{m!} \left[e^{\frac{t(b-\alpha+m)}{t_p}} E_{b+m-\alpha+1} \left(\frac{\alpha e^{-t/t_p}}{2} \right) - E_{b+m-\alpha+1} \left(\frac{\alpha}{2} \right) \right], \end{aligned} \quad (51)$$

where α and b are defined below Eq. (48), and $E_n(y) = \int_1^\infty dx x^{-n} e^{-xy}$ is the exponential integral function. Here, \mathcal{I}_2 is evaluated in Appendix B.2. In the long-time limit, both first and second terms go to zero if $A\sigma^2(\theta + 2t_p) < 2\sigma_0/3$; therefore, $\langle x^3 \rangle_{t \rightarrow \infty} = 0$.

Finally, we compute the fourth moment ($n = 4$)

$$\begin{aligned} \langle x^4 \rangle &= x_0^4 \langle f^{-4} \tau^0 \rangle + 12 x_0^2 \langle f^{-4} \tau^1 \rangle + 12 \langle f^{-4} \tau^2 \rangle \\ &= x_0^4 e^{-4\sigma_0 t} e^{-8\sigma^2 H_1(t)} + 12 x_0^2 e^{-4\sigma_0 t} e^{-8\sigma^2 H_1(t)} \int_0^t ds e^{2\sigma_0 s} e^{-2\sigma^2 [H_2(s,s) - 4H_2(t,s)]} + \\ &\quad + 12 e^{-4\sigma_0 t} e^{-8\sigma^2 H_1(t)} \int_0^t ds_1 \int_0^t ds_2 e^{2\sigma_0(s_1+s_2)} e^{-\sigma^2/2 [4 \sum_{m_1=1}^2 \sum_{m_2=1}^2 H_2(s_{m_1}, s_{m_2}) - 16 \sum_{m=1}^2 H_2(t, s_m)]} . \end{aligned} \quad (52)$$

While it is not straightforward to analyze the convergence criteria for the third integral, from the first two terms we find that these terms saturate at long times if $A\sigma^2(\theta + 2t_p) < \sigma_0/2$. We numerically checked that the fourth moment converges with this same condition. Thus, analyzing the first four moments, we find that these moments exist when $A\sigma^2(\theta + 2t_p) < 2\sigma_0/n$, where n is the order of the moment. We hypothesize that this is true for any n , as in the case of white noise limit $t_p \rightarrow 0$ [see Eq. (23)]. To verify expressions (46), (48), (51), and (52), we have performed numerical Langevin simulations. Figure 4 shows a good agreement of the analytical results for each moment with the numerical Langevin simulations.

5. Thermodynamics

In this work, we discuss a system where the stiffness of the harmonic trap is a fluctuating quantity. As a consequence of these temporal stochastic fluctuations, the particle is driven away from equilibrium. system, it is interesting to We now analyze thermodynamic quantities, such as work performed on the system and heat exchanged by the system with the heat bath, as functions of time.

We start by considering the internal energy of the particle $U(x, t; k)$, where k is the time-dependent control parameter. Taking a time-derivative of the internal energy gives the rate of net change of internal energy. This occurs due to rate of change of the particle's position and due to rate of change of the control parameter on a single stochastic trajectory level [61]:

$$\frac{dU(x, t; k)}{dt} = \underbrace{\frac{\partial U(x, t; k)}{\partial x} \dot{x}}_q + \underbrace{\frac{\partial U(x, t; k)}{\partial k} \dot{k}}_w , \quad (53)$$

where the first quantity on the right-hand side is the rate of heat entering in the system from the bath, while the second quantity is the rate of work performed on the system due to change of the control parameter k . (Notice that $q > 0$ and $w > 0$, respectively, correspond to the situation when heat flows from the bath to the system, and work is

performed on the particle.) For our system described in Eq. (2), the system's internal energy in the reduced unit is given by

$$U(x, t; k) = \frac{1}{2}[\sigma_0 + \sigma k(t)]x^2 . \quad (54)$$

Therefore, the work along a single stochastic trajectory follows from Eq. (53) as

$$w(t) = \sigma \int_0^t ds \frac{\dot{k}}{2} x^2 . \quad (55)$$

Notice that w goes to zero as $\sigma \rightarrow 0$, as it should be, since $\sigma \rightarrow 0$ corresponds to an equilibrium situation. Furthermore, the heat taken by the particle from the bath follows from Eq. (53) as

$$q(t) = \int_0^t ds [\sigma_0 + \sigma k(t)] x \dot{x} . \quad (56)$$

Henceforth, for convenience, we drop the explicit mention of the time-dependence of $U(x, t; k)$, $w(t)$ and $q(t)$, and simply write as $U(x; k)$, w and q .

Both work w and heat q are fluctuating quantities, that is, their values vary from one trajectory $[\{x, k\}]_{0 < t' \leq t}$ to another. Therefore, it would be interesting to compute the full fluctuations [probabilities density function (PDF)] of these quantities. However, the computation of PDFs is not straightforward. Nevertheless, we can exactly compute the average of these quantities for all time. (Notice that Ref. [59] discusses the entropy production only in the stationary state.)

In the following, we first show the calculation for the average work from Eq. (55). To this end, we perform an integration by parts

$$w = \frac{\sigma}{2} \left[k(s) V(s) \right]_0^t - \sigma \int_0^t ds \frac{1}{2} k(s) \dot{V} , \quad (57)$$

where we defined $V(t) \equiv x^2(t)$. The average work is obtained by performing the ensemble average over trajectories of x and k , i.e., $\mathcal{W} \equiv \langle w \rangle_{\{x, k\}}$.

We first perform the average over x for a given realization of $k(t)$. Assuming that the particle starts from a fixed location x_0 , we have

$$W = \frac{\sigma}{2} \left[k(t) \mathcal{V}(t) - k_0 V(0) \right] - \sigma \int_0^t ds k(s) \frac{\dot{\mathcal{V}}}{2} , \quad (58)$$

where we defined $W \equiv \langle w \rangle_{\{x\}}$ and $\mathcal{V}(t) \equiv \langle V(t) \rangle_{\{x\}}$, where \mathcal{V} is the second moment of the particle's position for a given realization of $k(t)$ starting from k_0 . Notice that the initial condition k_0 is distributed according to $p_{ss}(k_0)$ (5).

We proceed by multiplying x^2 on both sides of Fokker-Planck equation (33) and integrating from $x = -\infty$ to $x = +\infty$. This gives the time evolution of the second positional moment \mathcal{V} for each realization of $k(t)$:

$$\dot{\mathcal{V}}(t) = -2[\sigma_0 + \sigma k(t)] \mathcal{V}(t) + 2 . \quad (59)$$

Substituting $\dot{\mathcal{V}}(t)$ (59) on the right-hand side of Eq. (58), and performing the average over noise realization of $k(t)$, we obtain the average work

$$\mathcal{W} = \frac{\sigma}{2} \langle k(t) \mathcal{V}(t) \rangle_{\{k\}} + \sigma \sigma_0 \int_0^t ds \langle k(s) \mathcal{V}(s) \rangle_{\{k\}} + \sigma^2 \int_0^t ds \langle k^2(s) \mathcal{V}(s) \rangle_{\{k\}} , \quad (60)$$

where we substituted the stationary state $\langle k_0 \rangle = 0$. To compute the right-hand side of (60), we compute $\mathcal{V}(t)$ by solving Eq. (59). This yields

$$\mathcal{V}(t) = V(0) e^{-2[\sigma_0 t + \sigma \int_0^t ds k(s)]} + 2 \int_0^t dt' e^{-2[\sigma_0(t-t') + \sigma \int_{t'}^t ds k(s)]} , \quad (61)$$

where $V(0) = \mathcal{V}(0)$ since the particle starts from a fixed location $x = x_0$.

For simplicity, we now assume that the situation where the particle starts from the origin at time $t = 0$, i.e., $x_0 = 0$. Then, Eq. (61) becomes

$$\mathcal{V}(t) = 2 \int_0^t dt' e^{-2[\sigma_0(t-t') + \sigma \int_{t'}^t ds k(s)]} . \quad (62)$$

With this, we can compute the averages on the right-hand side of Eq. (60). The explicit calculations of each of the terms is cumbersome. Therefore, we relegate the computational details in the [Appendix C](#) and present here the final expressions as

$$\langle k(s) \mathcal{V}(s) \rangle_{\{k\}} = -4\sigma \int_0^s du H_3(u) e^{-2\sigma_0 u} e^{-2\sigma^2 H_1(u)} , \quad (63)$$

$$\langle k^2(s) \mathcal{V}(s) \rangle_{\{k\}} = 2 \int_0^s du \left[A \frac{(\theta + 2t_p)}{2t_p} + 4\sigma^2 H_3^2(u) \right] e^{-2\sigma_0 u} e^{-2\sigma^2 H_1(u)} , \quad (64)$$

where we defined

$$H_3(u) \equiv \frac{1}{2} A(\theta + 2t_p) \left(1 - e^{-\frac{u}{t_p}} \right) . \quad (65)$$

Substituting the results from Eqs. (63) and (64) into Eq. (60), we obtain the expression for the average work in the integral form. These integrals can be exactly calculated (see [Appendix C.1](#)). We here report the long-time result. In this long-time limit (for $b > 0$), the scaled average work approaches [see Eqs. (C.1), (C.23), (C.29), and (C.38)]

$$\begin{aligned} \lim_{t \rightarrow \infty} \mathcal{W}/t &= \sigma_0 e^{-\alpha} (-\alpha)^{-b} [-(b + \alpha) \Gamma(b) + \alpha \Gamma(b, -\alpha) + \Gamma(b + 1, -\alpha)] + \\ &\quad - \frac{e^{-\alpha} (-\alpha)^{-b}}{2t_p} [-(b + \alpha)(b + \alpha + 1) \Gamma(b) + \alpha(\alpha + 1) \Gamma(b, -\alpha) + \\ &\quad + 2\alpha \Gamma(b + 1, -\alpha) + \Gamma(b + 2, -\alpha)] , \end{aligned} \quad (66)$$

where α and b are defined below Eq. (48).

Next, we compute the average heat flow. The heat flow along a single stochastic trajectory (56) can be rewritten using Eq. (53) as

$$q = [U(x_t; k_t) - U(x_0; k_0)] - w \quad (67)$$

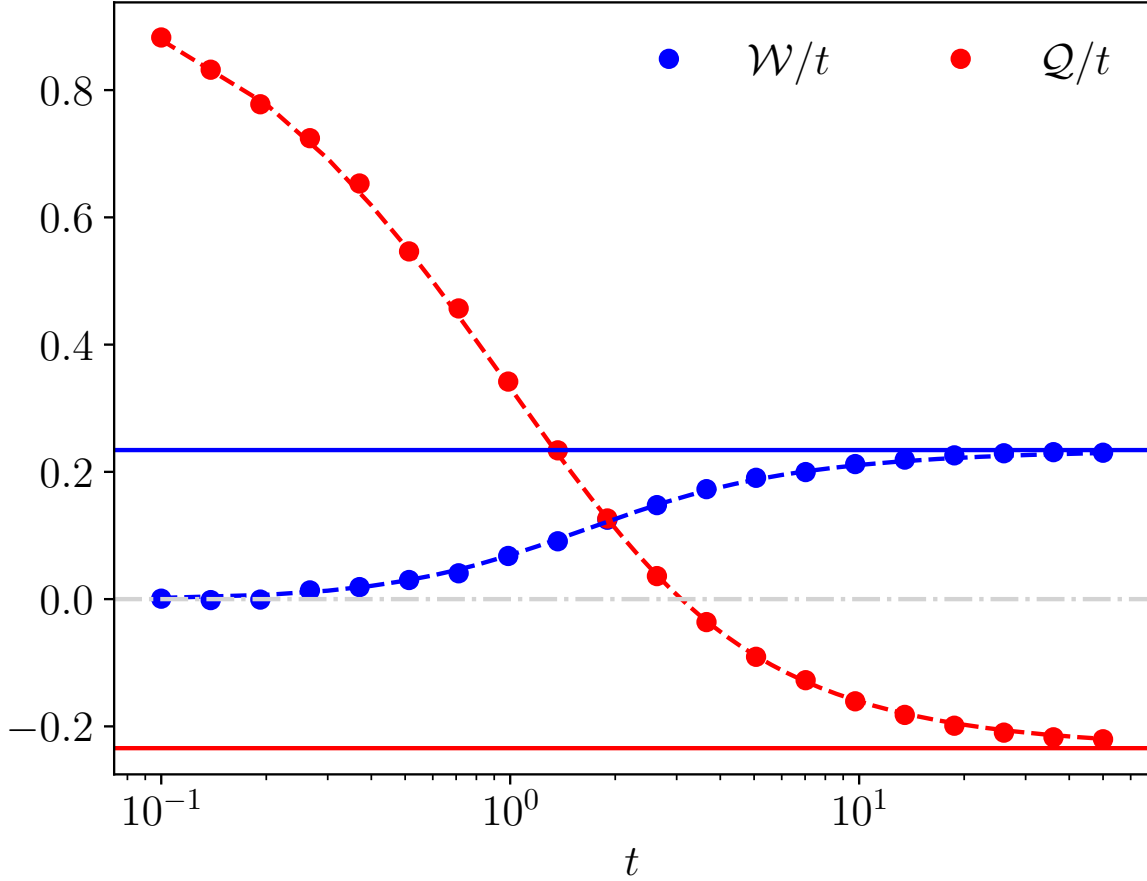


Figure 5. Average work per time (blue) and average heat per time (red), each as a function of observation time. Symbols: Numerical Langevin simulation. Dashed line: Analytical results (60) and (69). Solid horizontal line: Analytical result in the long-time limit (66) (blue) and the negative of the long-time limit expression (66) (red). The parameter are $A = 1.8$, $\theta = 2.5$, $t_p = 0.5$, $\sigma_0 = 1$, $\sigma = 0.23$, and $dt = 10^{-4}$. Number of realizations: 10^4 .

$$= \frac{\sigma_0}{2} [x_t^2 - x_0^2] + \frac{\sigma}{2} \int_0^t ds \, k(s) \dot{V} . \quad (68)$$

Averaging over an ensemble of trajectories $\{x\}_{0 \leq t' \leq t}$ (for fixed initial condition $x_0 = 0$) for each fixed trajectory of $k(t)$, subsequently substituting \dot{V} from Eq. (59) on the right-hand side. Then, we perform average over an ensemble of trajectories of $\{k\}_{0 \leq t' \leq t}$, and we obtain

$$\mathcal{Q} = \underbrace{\frac{\sigma_0}{2} \langle x^2 \rangle - \sigma \sigma_0 \int_0^t ds \, \langle k(s) \mathcal{V}(s) \rangle_{\{k\}}}_{\mathcal{W}_1} - \underbrace{\sigma^2 \int_0^t ds \, \langle k^2(s) \mathcal{V}(s) \rangle_{\{k\}}}_{\mathcal{W}_2} , \quad (69)$$

where $\langle x^2 \rangle$ is given in Eq. (48), and \mathcal{W}_1 and \mathcal{W}_2 are respectively evaluated in [Appendix C.1.2](#) and [Appendix C.1.3](#). In the long-time limit, $\langle x^2 \rangle$ is independent of t (49); therefore, $\lim_{t \rightarrow \infty} \mathcal{Q}/t$ is equal to the negative of $\lim_{t \rightarrow \infty} \mathcal{W}/t$ (66).

Figure 5 shows a good agreement of the analytical scaled average work (60), scaled average heat flow (69), their long-time expressions (66) and the negative of Eq. (66)] with the numerical Langevin simulations.

The results in Fig. 5 can be interpreted as follows. Initially, the system starts from $x_0 = 0$, which corresponds to a non-stationary state of the system (1). [Notice that the stationary state of the system is characterized by the joint distribution $P_{ss}(x_0, k_0)$.] At this initial stage, the average work done is negligible, and the internal energy of the system increases due to heat absorption from the environment—resulting in a positive heat rate.

As time progresses, the stochastic switching of stiffness $k(t)$ leads to an increase in the average work done on the system. However, the system simultaneously begins to dissipate heat back into the environment. Consequently, the heat rate decreases while the work rate increases over time.

In the long-time limit, the system reaches a stationary state where the rate of change of average internal energy goes to zero. At this point, the average work performed on the system due to stiffness switching is exactly balanced by the rate of heat dissipation into the environment.

6. Summary

In summary, we investigated an overdamped Brownian particle in one dimension, that is confined in a harmonic trap with fluctuating stiffness. The stiffness was modeled via a stationary Ornstein–Uhlenbeck process with correlation time t_p , i.e., the particle is confined in a fluctuating stiffness harmonic trap. In the absence of the heat bath (deterministic limit, i.e., temperature $T = 0$), we showed that the position’s fluctuations are log-normal distributed. Moreover, we showed that this probability density function can be represented in the large-deviation form [60].

We investigated the position’s fluctuations in the vanishing and long persistent time t_p limit. For the vanishing t_p case (i.e., white noise limit), the position distribution approaches a stationary power distribution with its tails decaying as $|x|^{-(1+2\sigma_0/a^2)}$ as $|x| \rightarrow \infty$, with a being the parameter controlling the stiffness’ fluctuation noise strength and $\sigma_0 > 0$. Herein, we showed the n th moment exist only if $a^2 < 2\sigma_0/n$. For the long persistent time t_p (i.e., quenched noise limit), the exact analytical expression in the integral form is obtained. In the limit of vanishing quenched disorder, we obtained an analytical expression of the probability density function using the saddle-point approach.

Further, for the case of finite non-zero t_p , we used the method of subordination [57, 58] to exactly compute the n th position’s moment and discussed the stationarity of these moments. It turned out that the moments exist only if $A\sigma^2(\theta + 2t_p) < 2\sigma_0/n$, which generalizes the condition of vanishing persistent time limit behavior.

From the thermodynamic point of view, this system is driven away from equilibrium by the stochastically fluctuating stiffness of the harmonic trap. To understand the energy flows associated with this system, we exactly computed the average work performed on

the particle and the heat exchanged by the particle with the heat bath for all times as well as in the steady state.

We here remark that our results can be easily generalized to the case when σ_0 [see Eq. (2a)] is itself a random quenched disorder parameter, i.e., $\sigma_0 \sim f(\sigma_0)$, with the normalized probability density function $f(\sigma_0)$. This can be done by performing a disorder average over σ_0 , similarly as we did in Sec. 4.2 for stiffness, k , behaving as a quenched random variable.

Our study opens several research avenues for future directions. It would be great to extend our analysis to compute the thermodynamic properties of Brownian particle in a trap with fluctuating both its minimum and stiffness (previously, researchers have investigated theoretically and experimentally the case of fluctuating trap's minimum [38, 39]). Another extension would be to generalize the results of a many particle system as in Ref. [53] to the case of trap's stiffness fluctuates according to a stationary Ornstein–Uhlenbeck process [Eq. (1b) and (5)] or more generally to stiffness randomly fluctuating in an interval, $k(t) \in [k_-, k_+]$, with a constant rate. Further extension in the direction of many particle system would be to investigate the heat flow in harmonic chain [62, 63] of fluctuating interactions. Finally, we emphasize that our results can be tested in an experiment by extending Ref. [64] to stochastically switching the intensity of laser beam confining the particle.

Acknowledgments

D.G. thanks Gregory Schehr and Jan Meibohm for many fruitful discussions. D.G. acknowledges the support from the Alexander von Humboldt foundation.

Appendix A. Derivation of Fokker-Planck equation for white noise stiffness

In general, the Fokker-Planck equation is given by [65]

$$\frac{\partial P(x, t|x_0)}{\partial t} = -\frac{\partial}{\partial x} \left[\frac{\langle \Delta x \rangle}{\Delta t} \bigg|_{\Delta t \rightarrow 0} P(x, t|x_0) \right] + \frac{1}{2} \frac{\partial^2}{\partial x^2} \left[\frac{\langle \Delta x^2 \rangle}{\Delta t} \bigg|_{\Delta t \rightarrow 0} P(x, t|x_0) \right]. \quad (\text{A.1})$$

For the white noise stiffness [Sec. 4.1 and Eq. (7)], i.e., the temporal correlation of the stiffness are delta correlated, we have the following stochastic differential equation (SDE):

$$\dot{x}(t) = -(\sigma_0 + a\xi(t))x(t) + \sqrt{2}\eta(t) \quad (\text{A.2})$$

where $\langle \eta(t)\eta(t') \rangle = \delta(t - t')$ and $\langle \xi(t)\xi(t') \rangle = \delta(t - t')$, and $a \equiv \sigma\sqrt{A\theta}$. We now aim to compute the Fokker-Planck equation corresponding to above SDE. To this end, we compute the average $\langle \Delta x(t) \rangle \equiv \langle x(t + \Delta) - x(t) \rangle / \Delta t$ and $\langle [\Delta x(t)]^2 \rangle / \Delta t$ in the limit $\Delta t \rightarrow 0$.

We first discretize the Langevin dynamics (A.2)

$$\begin{aligned}\Delta x(t) &= \sqrt{2} \int_t^{t+\Delta t} ds \eta(s) - \int_t^{t+\Delta t} ds [\sigma_0 + a\xi(s)]x(s) \\ &= \sqrt{2} \int_t^{t+\Delta t} ds \eta(s) - x(\tau) \int_t^{t+\Delta t} ds [\sigma_0 + a\xi(s)] ,\end{aligned}\quad (\text{A.3})$$

where we used the mean value theorem in the second integral for any $\tau \in [t, t + \Delta t]$. Now since $\xi(t)$ is a stochastic quantity, the choice of τ matters. Let us say $x(\tau) \equiv \alpha x(t + \Delta t) + (1 - \alpha)x(t) = x(t) + \alpha \Delta x(t)$ for any α . Specifically, $\alpha = 0, 1/2, 1$, respectively, correspond to Ito, Stratonovich, and anti-Ito.

For a small Δt , we can approximate the above integrals, yielding

$$\Delta x(t) = \underbrace{\sqrt{2} \int_t^{t+\Delta t} ds \eta(s)}_{I_0} - \underbrace{[x(t) + \alpha \Delta x(t)][\sigma_0 \Delta t + a \int_t^{t+\Delta t} ds \xi(s)]}_{I_1} . \quad (\text{A.4})$$

Let us now focus on the following integral:

$$I_1 = [x(t) + \alpha \Delta x(t)][\sigma_0 \Delta t + a \int_t^{t+\Delta t} ds \xi(s)] . \quad (\text{A.5})$$

Substituting $\Delta x(t)$ from the above equation, we get

$$\begin{aligned}I_1 &= x(t) \left[\sigma_0 \Delta t + a \int_t^{t+\Delta t} ds \xi(s) \right] + \alpha \left[\sigma_0 \Delta t + a \int_t^{t+\Delta t} ds \xi(s) \right] \left[\sqrt{2} \int_t^{t+\Delta t} ds' \eta(s') \right. \\ &\quad \left. - [x(t) + \alpha \Delta x(t)][\sigma_0 \Delta t + a \int_t^{t+\Delta t} ds' \xi(s')] \right]\end{aligned}\quad (\text{A.6})$$

Averaging over noises, we get

$$\begin{aligned}\langle I_1 \rangle &= \Delta t \sigma_0 x(t) - \left\langle \alpha x(t) [\sigma_0 \Delta t + a \int_t^{t+\Delta t} ds \xi(s)] [\sigma_0 \Delta t + a \int_t^{t+\Delta t} ds' \xi(s')] \right\rangle \\ &= \Delta t [\sigma_0 - \alpha a^2] x(t)\end{aligned}\quad (\text{A.7})$$

where we dropped terms higher order than Δt including Δx (which will eventually gives terms higher order than Δt). This implies

$$\langle \Delta x(t) \rangle = -\Delta t [\sigma_0 - \alpha a^2] x(t) \quad (\text{A.8})$$

yielding the first term in the Fokker-Planck equation: $\lim_{\Delta t \rightarrow 0} \langle \Delta x \rangle / \Delta t$.

Proceeding similarly as above, we compute the second moment:

$$\begin{aligned}\langle [\Delta x(t)]^2 \rangle &= \left\langle 2 \int_t^{t+\Delta t} ds' \eta(s) \eta(s') + [x(t) + \alpha \Delta x(t)]^2 [\sigma_0^2 \Delta t^2 + a^2 \int_t^{t+\Delta t} ds' \xi(s) \xi(s')] \right. \\ &\quad \left. + 2 \Delta t \sigma_0 a \int_t^{t+\Delta t} ds \xi(s) \right\rangle .\end{aligned}\quad (\text{A.9})$$

From this, we obtain

$$\langle [\Delta x(t)]^2 \rangle = [2 + x(t)^2 a^2] \Delta t \quad (\text{A.10})$$

which gives the second term in the Fokker-Planck equation: $\lim_{\Delta t \rightarrow 0} \langle \Delta x^2 \rangle / \Delta t$.

Using Eq. (A.1), the Fokker-Planck equation corresponding to SDE (A.2) results as

$$\frac{\partial P(x, t|x_0)}{\partial t} = \frac{\partial}{\partial x} \left[(\sigma_0 - \alpha a^2) x P(x, t|x_0) \right] + \frac{\partial^2}{\partial x^2} \left[(1 + a^2 x^2 / 2) P(x, t|x_0) \right], \quad (\text{A.11})$$

where the second term (proportional to a^2) in each of the square brackets on the right-hand side is due to the white noise stiffness.

Appendix B. Evaluation of integrals \mathcal{I}_1 (47) and \mathcal{I}_1 (50)

Appendix B.1. Calculation of \mathcal{I}_1

$$\begin{aligned} \mathcal{I}_1 &= \int_0^t ds \, e^{-2\sigma_0 s} e^{-2\sigma^2 H_1(s)} \\ &= e^{-\alpha} \int_0^t ds \, e^{-s/t_p(2\sigma_0 t_p - \alpha)} e^{\alpha e^{-s/t_p}} \end{aligned} \quad (\text{B.1})$$

where we defined

$$\alpha \equiv 2\sigma^2 A t_p (\theta + 2t_p) . \quad (\text{B.2})$$

Substituting $z = e^{-s/t_p}$, we get

$$\begin{aligned} \mathcal{I}_1 &= t_p e^{-\alpha} \int_{e^{-t/t_p}}^1 dz \, z^{a-1} e^{\alpha z} \\ &= t_p e^{-\alpha} (-\alpha)^{-a} \left[\Gamma\left(a, -e^{-\frac{t}{t_p}} \alpha\right) - \Gamma(a, -\alpha) \right], \end{aligned} \quad (\text{B.3})$$

where $\Gamma(a, z) = \int_z^\infty x^{a-1} e^{-x}$ is the incomplete gamma function. The integral is evaluated for $t_p > 0$ and $a = 2\sigma_0 t_p - \alpha$. In the limit $t \rightarrow \infty$, $\Gamma\left(a, -e^{-\frac{t}{t_p}} \alpha\right)$ becomes $\Gamma(a)$ for $a > 0$.

$$\mathcal{I}_1 = t_p e^{-\alpha} (-\alpha)^{-a} [\Gamma(a) - \Gamma(a, -\alpha)] , \quad (\text{B.4})$$

Appendix B.2. \mathcal{I}_2

$$\mathcal{I}_2 = \int_0^t ds e^{2\sigma_0 s} e^{-2\sigma^2 [H_2(s, s) - 3H_2(t, s)]} . \quad (\text{B.5})$$

Substituting $z = e^{-s/t_p}$, we get

$$\mathcal{I}_2 = t_p e^{\alpha/2} e^{-\frac{3\alpha}{2} e^{-t/t_p}} \int_{e^{-t/t_p}}^1 dz \, z^{2\alpha - 2\sigma_0 t_p - 1} e^{-\alpha z/2} e^{\frac{3\alpha}{2} \frac{e^{-t/t_p}}{z}} \quad (\text{B.6})$$

$$= t_p e^{\alpha/2} e^{-\frac{3\alpha}{2} e^{-t/t_p}} \int_{e^{-t/t_p}}^1 dz z^{\alpha-a-1} e^{-\alpha z/2} e^{\frac{3\alpha}{2} \frac{e^{-t/t_p}}{z}} \quad (\text{B.7})$$

$$= t_p e^{\alpha/2} e^{-\frac{3\alpha}{2} e^{-t/t_p}} \sum_{m=0}^{\infty} \frac{(3\alpha/2)^m e^{-mt/t_p}}{m!} \int_{e^{-t/t_p}}^1 dz z^{\alpha-a-1-m} e^{-\alpha z/2} \quad (\text{B.8})$$

$$= t_p e^{\alpha/2} e^{-\frac{3\alpha}{2} e^{-t/t_p}} \sum_{m=0}^{\infty} \frac{(3\alpha/2)^m e^{-mt/t_p}}{m!} \left[e^{\frac{t(a-\alpha+m)}{t_p}} E_{a+m-\alpha+1} \left(\frac{\alpha e^{-\frac{t}{t_p}}}{2} \right) - E_{a+m-\alpha+1} \left(\frac{\alpha}{2} \right) \right], \quad (\text{B.9})$$

where $E_n(y) = \int_1^\infty dx x^{-n} e^{-xy}$ is the exponential integral function.

Appendix C. Calculations of average \mathcal{W}

$$\mathcal{W} = \underbrace{\frac{\sigma}{2} \langle k(t) \mathcal{V}(t) \rangle_{\{k\}}}_{\mathcal{W}_0} + \underbrace{\sigma \sigma_0 \int_0^t ds \langle k(s) \mathcal{V}(s) \rangle_{\{k\}}}_{\mathcal{W}_1} + \underbrace{\sigma^2 \int_0^t ds \langle k^2(s) \mathcal{V}(s) \rangle_{\{k\}}}_{\mathcal{W}_2}, \quad (\text{C.1})$$

To compute this average work, we have to compute the following annealed averages, i.e., averages over the stochastic trajectories of $k(t)$

$$A_n = \langle k^n(u) \mathcal{V}(u) \rangle_{\{k(t)\}}, \quad (\text{C.2})$$

for $n = 1, 2$. For convenience, in the following, we drop the subscript $\{k(t)\}$.

We aim to compute the average work for a fixed initial condition $x_0 = 0$. The second moment for a given realization of $k(t)$ is the solution of Eq. (62)

$$\mathcal{V}(u) = 2 \int_0^u ds e^{-2\sigma_0(u-s)} e^{-2\sigma \int_s^u ds' k(s')} . \quad (\text{C.3})$$

Then, the average for $n = 1$ in Eq. (C.2) is

$$\langle k(u) \mathcal{V}(u) \rangle = 2 \int_0^u ds e^{-2\sigma_0(u-s)} \left\langle k(u) e^{-2\sigma \int_s^u ds' k(s')} \right\rangle . \quad (\text{C.4})$$

Since the average of $k(t)$ in the stationary-state (5) is zero, the non-zero contributions arise from the odd-multiple terms of $k(t)$ from the expansion of the exponential

$$\begin{aligned} \left\langle k(u) e^{-2\sigma \int_s^u ds' k(s')} \right\rangle &= \left\langle k(u) \left[-2\sigma \int_s^u dm_1 k(m_1) + \right. \right. \\ &\quad - \frac{(2\sigma)^3}{3!} \int_s^u dm_1 \int_s^u dm_2 \int_s^u dm_3 k(m_1) k(m_2) k(m_3) + \\ &\quad \left. \left. - \frac{(2\sigma)^5}{5!} \int_s^u dm_1 \int_s^u dm_2 \int_s^u dm_3 \int_s^u dm_4 \int_s^u dm_5 k(m_1) k(m_2) k(m_3) k(m_4) k(m_5) + \dots \right] \right\rangle \\ &\equiv T_1^{(1)}(s, u) + T_2^{(1)}(s, u) + T_3^{(1)}(s, u), \end{aligned} \quad (\text{C.5})$$

where

$$T_1^{(1)} = -2\sigma \int_s^u dm_1 \langle k(u)k(m_1) \rangle, \quad (\text{C.6})$$

$$\begin{aligned} T_2^{(1)} &= -\frac{(2\sigma)^3}{3!} \int_s^u dm_1 \int_s^u dm_2 \int_s^u dm_3 \langle k(t)k(m_1)k(m_2)k(m_3) \rangle \\ &= -3\frac{(2\sigma)^3}{3!} \int_s^u dm_1 \int_s^u dm_2 \int_s^u dm_3 \langle k(t)k(m_1) \rangle \langle k(m_2)k(m_3) \rangle \\ &= T_1^{(1)} \frac{(2\sigma)^2}{2} \int_s^u dm_1 \int_s^u dm_2 \langle k(m_1)k(m_2) \rangle, \end{aligned} \quad (\text{C.7})$$

$$\begin{aligned} T_3^{(1)} &= -\frac{(2\sigma)^5}{5!} \int_s^u dm_1 \int_s^u dm_2 \int_s^u dm_3 \int_s^u dm_4 \int_s^u dm_5 \langle k(t)k(m_1)k(m_2)k(m_3)k(m_4)k(m_5) \rangle \\ &= -15\frac{(2\sigma)^5}{5!} \int_s^u dm_1 \int_s^u dm_2 \int_s^u dm_3 \int_s^u dm_4 \int_s^u dm_5 \langle k(t)k(m_1) \rangle \langle k(m_2)k(m_3) \rangle \langle k(m_4)k(m_5) \rangle \\ &= T_1^{(1)} \frac{\sigma^2}{2!} \int_{t'}^t dm_1 \int_s^u dm_2 \int_s^u dm_3 \int_s^u dm_4 \langle k(m_2)k(m_3) \rangle \langle k(m_4)k(m_5) \rangle, \end{aligned} \quad (\text{C.8})$$

where we used the Wick's theorem to simplify the higher-point correlations into two-point correlations. Thus, Eq. (C.4) becomes

$$\begin{aligned} \langle k(u)\mathcal{V}(u) \rangle &= 2 \int_0^u ds e^{-2(\sigma_0(u-s))} \sum_{i=1}^3 T_i^{(1)}(s, u) \\ &= 2 \int_0^u ds e^{-2\sigma_0(u-s)} T_1^{(1)}(s, u) e^{2\sigma^2 \int_s^u dm_1 \int_s^u dm_2 \langle k(m_1)k(m_2) \rangle} \\ &= -4\sigma \int_0^u ds H_3(u-s) e^{-2\sigma_0(u-s)} e^{-2\sigma^2 H_1(u-s)} \\ &= -4\sigma \int_0^u ds H_3(u) e^{-2\sigma_0 u} e^{-2\sigma^2 H_1(u)}, \end{aligned} \quad (\text{C.9})$$

where we defined

$$H_1(u) \equiv At_p(\theta + 2t_p)(1 - u/t_p - e^{-u/t_p}), \quad (\text{C.10})$$

$$H_3(u) \equiv \frac{1}{2}A(\theta + 2t_p) \left(1 - e^{-\frac{u}{t_p}}\right). \quad (\text{C.11})$$

Let us now compute the average for $n = 2$ in Eq. (C.2)

$$\langle k^2(u)\mathcal{V}(u) \rangle = 2 \int_0^u ds e^{-2\sigma_0(u-s)} \left\langle k^2(u) e^{-2\sigma \int_s^u ds' k(s')} \right\rangle. \quad (\text{C.12})$$

Similar to the calculation for $n = 1$, here the even multiple of $k(t)$ terms from the exponential contribute; therefore,

$$\left\langle k^2(u) e^{-2\sigma \int_s^u ds' k(s')} \right\rangle = \left\langle k^2(u) \left[1 + \frac{(2\sigma)^2}{2!} \int_{s_1}^u dm_1 \int_{s_1}^u dm_2 k(m_1)k(m_2) + \right. \right.$$

$$\begin{aligned}
& + \frac{(2\sigma)^4}{4!} \int_{s_1}^u dm_1 \int_{s_1}^u dm_2 \int_{s_1}^u dm_3 \int_{s_1}^u dm_4 k(m_1)k(m_2)k(m_3)k(m_4) + \dots \Bigg] \\
& \equiv T_1^{(2)}(s, u) + T_2^{(2)}(s, u) + T_3^{(2)}(s, u) , \tag{C.13}
\end{aligned}$$

where

$$T_1^{(2)} = \langle k^2(u) \rangle , \tag{C.14}$$

$$\begin{aligned}
T_2^{(2)} &= \frac{(2\sigma)^2}{2!} \int_s^u dm_1 \int_s^u dm_2 \langle k^2(u)k(m_1)k(m_2) \rangle \\
&= T_1^{(2)} \frac{(2\sigma)^2}{2} \int_s^u dm_1 \int_s^u dm_2 \langle k(m_1)k(m_2) \rangle + (2\sigma)^2 \left[\int_s^u ds \langle k(u)k(s) \rangle \right]^2 , \tag{C.15}
\end{aligned}$$

$$\begin{aligned}
T_3^{(2)} &= 3T_1^{(2)} \frac{(2\sigma)^4}{4!} \left[\int_s^u dm_1 \int_{s_1}^u dm_2 \langle k(m_1)k(m_2) \rangle \right]^2 + 12 \frac{(2\sigma)^4}{4!} \left[\int_s^u dm_1 \langle k(u)k(m_1) \rangle \right]^2 \times \\
&\times \left[\int_s^u dm_3 \int_s^u dm_4 \langle k(m_3)k(m_4) \rangle \right] \\
&= T_1^{(2)} \frac{((2\sigma)^2/2)^2}{2!} \left[\int_s^u dm_1 \int_s^u dm_2 \langle k(m_1)k(m_2) \rangle \right]^2 + \frac{(2\sigma)^4}{2} \left[\int_s^u dm_1 \langle k(u)k(m_1) \rangle \right]^2 \times \\
&\times \left[\int_s^u dm_3 \int_s^u dm_4 \langle k(m_3)k(m_4) \rangle \right] . \tag{C.16}
\end{aligned}$$

Therefore, Eq. (C.12) becomes

$$\begin{aligned}
\langle k^2(u) \mathcal{V}(u) \rangle &= 2 \int_0^u ds e^{-2\sigma_0(u-s)} \sum_{i=1}^3 T_i^{(2)}(s, u) \\
&= 2 \int_0^u ds e^{-2\sigma_0(u-s)} \left[T_1^{(2)} + 4\sigma^2 \left(\int_s^u dm_1 \langle k(u)k(m_1) \rangle \right)^2 \right] \times \\
&\times \exp \left[2\sigma^2 \int_s^u dm_1 \int_s^u dm_2 \langle k(m_1)k(m_2) \rangle \right] \\
&= 2 \int_0^u ds \left[A \frac{(\theta + 2t_p)}{2t_p} + 4\sigma^2 H_3^2(u-s) \right] e^{-2\sigma_0(u-s)} e^{-2\sigma^2 H_1(u-s)} \\
&= 2 \int_0^u ds \left[A \frac{(\theta + 2t_p)}{2t_p} + 4\sigma^2 H_3^2(u) \right] e^{-2\sigma_0 u} e^{-2\sigma^2 H_1(u)} , \tag{C.17}
\end{aligned}$$

where $H_1(u)$ and $H_3(u)$ are defined in Eqs. (C.10) and (C.11).

Appendix C.1. Calculations of $\mathcal{W}_{0,1,2}$ (C.1)

In the following, we calculate the integrals involving in $\mathcal{W}_{0,1,2}$ (C.1).

Appendix C.1.1. Calculation of \mathcal{W}_0 : Here, we calculate \mathcal{W}_0 , where we need to compute the following average [see Eq. (C.9)]

$$\langle k(s) \mathcal{V}(s) \rangle_{\{k\}} = -4\sigma \int_0^s du H_3(u) e^{-2\sigma_0 u} e^{-2\sigma^2 H_1(u)} , \tag{C.18}$$

where $H_1(u)$ and $H_3(u)$ are respectively given in Eqs. (C.10) and (C.11).

We simplify the above integral (C.18)

$$\langle k(s)\mathcal{V}(s) \rangle_{\{k\}} = -\frac{\alpha}{\sigma t_p} e^{-\alpha} \int_0^s du \left(e^{-u/t_p(2\sigma_0 t_p - \alpha)} - e^{-\frac{u}{t_p}(2\sigma_0 t_p + 1 - \alpha)} \right) e^{\alpha e^{-u/t_p}}, \quad (\text{C.19})$$

where, for convenience, we defined $\alpha \equiv 2\sigma^2 A t_p (\theta + 2t_p)$.

Substituting $e^{-u/t_p} = z$, we get

$$\begin{aligned} \langle k(s)\mathcal{V}(s) \rangle_{\{k\}} &= \frac{\alpha}{\sigma} e^{-\alpha} \int_1^{e^{-s/t_p}} dz \left[z^{(2\sigma_0 t_p - \alpha - 1)} - z^{(2\sigma_0 t_p - \alpha)} \right] e^{\alpha z} \\ &= \frac{e^{-\alpha} (-\alpha)^{-b}}{\sigma} \left[\alpha \Gamma(b, -\alpha) + \Gamma(b+1, -\alpha) - \alpha \Gamma\left(b, -e^{-\frac{s}{t_p}} \alpha\right) - \Gamma\left(b+1, -e^{-\frac{s}{t_p}} \alpha\right) \right], \end{aligned} \quad (\text{C.20})$$

where $\Gamma(b, z) = \int_z^\infty dx x^{b-1} e^{-x}$ is the incomplete gamma function, and we again defined

$$b \equiv 2\sigma_0 t_p - \alpha. \quad (\text{C.21})$$

The right-hand side of Eq. (C.20) in the long-time limit converges for $b > 0$:

$$\lim_{t \rightarrow \infty} \langle k(t)\mathcal{V}(t) \rangle_{\{k\}} \rightarrow \frac{e^{-\alpha} (-\alpha)^{-b}}{\sigma} [-(b+\alpha)\Gamma(b) + \alpha\Gamma(b, -\alpha) + \Gamma(b+1, -\alpha)]. \quad (\text{C.22})$$

Therefore, the contribution from the scaled average \mathcal{W}_0/t in the long time limit is:

$$\lim_{t \rightarrow \infty} \mathcal{W}_0/t = 0. \quad (\text{C.23})$$

Appendix C.1.2. Calculation of \mathcal{W}_1 : To evaluate the second term in \mathcal{W}_1 in Eq. (C.1) we see that

$$\begin{aligned} \mathcal{W}_1 &= \sigma \sigma_0 \int_0^t ds \langle k(s)\mathcal{V}(s) \rangle_{\{k\}} \\ &= -\frac{\alpha \sigma_0}{t_p} e^{-\alpha} \int_0^t ds \int_0^s du \left(e^{-2\sigma_0 u} - e^{-\frac{u}{t_p}(2\sigma_0 t_p + 1)} \right) e^{\alpha u/t_p} e^{\alpha e^{-u/t_p}}, \end{aligned} \quad (\text{C.24})$$

where we used Eq. (C.19).

Swapping the order of integration on the right-hand side of Eq. (C.24), we get

$$\mathcal{W}_1 = -\frac{\alpha \sigma_0}{t_p} e^{-\alpha} \int_0^t du (t-u) \left(e^{-2\sigma_0 u} - e^{-\frac{u}{t_p}(2\sigma_0 t_p + 1)} \right) e^{\alpha u/t_p} e^{\alpha e^{-u/t_p}} \quad (\text{C.25})$$

$$= \underbrace{\sigma \sigma_0 t \langle k(t)\mathcal{V}(t) \rangle_{\{k\}}}_{\mathcal{W}_1^{(1)}} + \underbrace{\frac{\alpha \sigma_0}{t_p} e^{-\alpha} \int_0^t du u \left(e^{-2\sigma_0 u} - e^{-\frac{u}{t_p}(2\sigma_0 t_p + 1)} \right) e^{\alpha u/t_p} e^{\alpha e^{-u/t_p}}}_{\mathcal{W}_1^{(2)}}. \quad (\text{C.26})$$

We evaluate $\mathcal{W}_1^{(1)}$ at time t using Eq. (C.20), while we substitute $z = e^{-u/t_p}$ in $\mathcal{W}_1^{(2)}$ (C.26); this gives

$$\mathcal{W}_1^{(2)} = \alpha \sigma_0 t_p e^{-\alpha} \int_1^{e^{-t/t_p}} dz \ln z \left[z^{(2\sigma_0 t_p - \alpha - 1)} - z^{(2\sigma_0 t_p - \alpha)} \right] e^{\alpha z}$$

$$\begin{aligned}
&= e^{-\alpha} \sigma_0 (-\alpha)^{-b} \left[t_p \left\{ \alpha G_{2,3}^{3,0} \left(-\alpha \left| \begin{matrix} 1, 1 \\ 0, 0, b \end{matrix} \right. \right) + G_{2,3}^{3,0} \left(-\alpha \left| \begin{matrix} 1, 1 \\ 0, 0, b+1 \end{matrix} \right. \right) + \right. \right. \\
&\quad \left. \left. - \alpha G_{2,3}^{3,0} \left(-e^{-\frac{t}{t_p}} \alpha \left| \begin{matrix} 1, 1 \\ 0, 0, b \end{matrix} \right. \right) - G_{2,3}^{3,0} \left(-e^{-\frac{t}{t_p}} \alpha \left| \begin{matrix} 1, 1 \\ 0, 0, b+1 \end{matrix} \right. \right) \right\} + \right. \\
&\quad \left. + t \left(\alpha \Gamma \left(b, -e^{-\frac{t}{t_p}} \alpha \right) + \Gamma \left(b+1, -e^{-\frac{t}{t_p}} \alpha \right) \right) \right], \tag{C.27}
\end{aligned}$$

where $G(\dots)$ is the Meijer G function.

Further, the integral $\mathcal{W}_1^{(2)}$ (C.27) in the long-time limit converges (and becomes independent of t) for $b > 0$, and this gives

$$\lim_{t \rightarrow \infty} \mathcal{W}_1^{(2)} = e^{-\alpha} \alpha \sigma_0 t_p \left(\frac{{}_2F_2(b, b; b+1, b+1; \alpha)}{b^2} - \frac{{}_2F_2(b+1, b+1; b+2, b+2; \alpha)}{(b+1)^2} \right), \tag{C.28}$$

where ${}_pF_q(b_1; b_2; z)$ is the generalized hypergeometric function.

Thus, from Eq. (C.26), we see that the dominant contribution to \mathcal{W}_1/t in the long-time limit comes from $\mathcal{W}_1^{(1)}$ (for $b > 0$), yielding

$$\lim_{t \rightarrow \infty} \mathcal{W}_1/t = \sigma_0 e^{-\alpha} (-\alpha)^{-b} [-(b+\alpha)\Gamma(b) + \alpha\Gamma(b, -\alpha) + \Gamma(b+1, -\alpha)] \tag{C.29}$$

Appendix C.1.3. Calculations of \mathcal{W}_2

$$\mathcal{W}_2 = \sigma^2 \int_0^t ds \langle k^2(s) \mathcal{V}(s) \rangle_{\{k\}} \tag{C.30}$$

$$= \mathcal{W}_2^{(1)} + \mathcal{W}_2^{(2)}, \tag{C.31}$$

where we substituted the expression (C.17) in Eq. (C.30), and then, substitute $z = e^{-s/t_p}$. This leads to the following integrals

$$\mathcal{W}_2^{(1)} \equiv -\frac{\alpha}{2t_p} e^{-\alpha t} \int_0^{e^{-t/t_p}} dz [(1+\alpha)z^{b-1} + \alpha(z^{b+1} - 2z^b)] e^{\alpha z}, \tag{C.32}$$

$$\mathcal{W}_2^{(2)} \equiv -\frac{\alpha}{2} e^{-\alpha} \int_0^{e^{-t/t_p}} dz \ln z [(1+\alpha)z^{b-1} + \alpha(z^{b+1} - 2z^b)] e^{\alpha z}, \tag{C.33}$$

where α is defined below Eq. (C.19).

Computing $\mathcal{W}_2^{(1)}$ and $\mathcal{W}_2^{(2)}$, we get

$$\begin{aligned}
\mathcal{W}_2^{(1)} &= -\frac{te^{-\alpha}(-\alpha)^{-b}}{2t_p} \left[\Gamma(b+2, -\alpha) + \alpha \left\{ (\alpha+1)\Gamma(b, -\alpha) + 2\Gamma(b+1, -\alpha) + \right. \right. \\
&\quad \left. \left. - (\alpha+1)\Gamma\left(b, -e^{-\frac{t}{t_p}}\alpha\right) - 2\Gamma\left(b+1, -e^{-\frac{t}{t_p}}\alpha\right) \right\} - \Gamma\left(b+2, -e^{-\frac{t}{t_p}}\alpha\right) \right], \tag{C.34}
\end{aligned}$$

$$\begin{aligned}
\mathcal{W}_2^{(2)} &= -\frac{e^{-\alpha}(-\alpha)^{-b}}{2t_p} \left[-\alpha^2 t_p G_{2,3}^{3,0} \left(-e^{-\frac{t}{t_p}} \alpha \left| \begin{matrix} 1, 1 \\ 0, 0, b \end{matrix} \right. \right) - \alpha t_p G_{2,3}^{3,0} \left(-e^{-\frac{t}{t_p}} \alpha \left| \begin{matrix} 1, 1 \\ 0, 0, b \end{matrix} \right. \right) \right. \\
&\quad \left. - 2\alpha t_p G_{2,3}^{3,0} \left(-e^{-\frac{t}{t_p}} \alpha \left| \begin{matrix} 1, 1 \\ 0, 0, b+1 \end{matrix} \right. \right) - t_p G_{2,3}^{3,0} \left(-e^{-\frac{t}{t_p}} \alpha \left| \begin{matrix} 1, 1 \\ 0, 0, b+2 \end{matrix} \right. \right) + \right.
\end{aligned}$$

$$\begin{aligned}
& -(\alpha+1)\alpha^2 t_p G_{2,3}^{3,0} \left(-\alpha \left| \begin{array}{c} 0,0 \\ -1,-1,b-1 \end{array} \right. \right) - 2\alpha^2 t_p G_{2,3}^{3,0} \left(-\alpha \left| \begin{array}{c} 0,0 \\ -1,-1,b \end{array} \right. \right) + \\
& -\alpha t_p G_{2,3}^{3,0} \left(-\alpha \left| \begin{array}{c} 0,0 \\ -1,-1,b+1 \end{array} \right. \right) + \alpha^2 t \Gamma \left(b, -e^{-\frac{t}{t_p}} \alpha \right) + \alpha t \Gamma \left(b, -e^{-\frac{t}{t_p}} \alpha \right) + \\
& + 2\alpha t \Gamma \left(b+1, -e^{-\frac{t}{t_p}} \alpha \right) + t \Gamma \left(b+2, -e^{-\frac{t}{t_p}} \alpha \right) \Big]. \tag{C.35}
\end{aligned}$$

Substituting these $\mathcal{W}_2^{(1),(2)}$ in Eq. (C.31) gives \mathcal{W}_2 .

In the long-time limit, both $\mathcal{W}_2^{(1)}$ and $\mathcal{W}_2^{(2)}$ converge and behave as (for $b > 0$)

$$\begin{aligned}
\mathcal{W}_2^{(1)} = & -\frac{te^{-\alpha}(-\alpha)^{-b}}{2t_p} [-(b+\alpha)(b+\alpha+1)\Gamma(b) + \alpha(\alpha+1)\Gamma(b, -\alpha) + \\
& + 2\alpha\Gamma(b+1, -\alpha) + \Gamma(b+2, -\alpha)] , \tag{C.36}
\end{aligned}$$

$$\begin{aligned}
\mathcal{W}_2^{(2)} = & -\frac{1}{2}e^{-\alpha}\alpha \left[\alpha\Gamma(b+2)^2 \left({}_2\tilde{F}_2(b+2, b+2; b+3, b+3; \alpha) + \right. \right. \\
& \left. \left. - \frac{{}_2\tilde{F}_2(b+1, b+1; b+2, b+2; \alpha)}{(b+1)^2} \right) + \frac{(\alpha+1){}_2F_2(b, b; b+1, b+1; \alpha)}{b^2} \right] . \tag{C.37}
\end{aligned}$$

Therefore, in the long-time limit, the dominant contribution to \mathcal{W}_2/t comes from $\mathcal{W}_2^{(1)}$ (C.36)

$$\begin{aligned}
\lim_{t \rightarrow \infty} \mathcal{W}_2/t = & -\frac{e^{-\alpha}(-\alpha)^{-b}}{2t_p} [-(b+\alpha)(b+\alpha+1)\Gamma(b) + \alpha(\alpha+1)\Gamma(b, -\alpha) + \\
& + 2\alpha\Gamma(b+1, -\alpha) + \Gamma(b+2, -\alpha)] . \tag{C.38}
\end{aligned}$$

References

- [1] Seifert U 2012 *Reports on Progress in Physics* **75** 126001 URL <https://dx.doi.org/10.1088/0034-4885/75/12/126001>
- [2] Shiraishi N 2023 *Fundamental Theories of Physics*. Springer, Singapore
- [3] Van Kampen N G 1992 *Stochastic processes in physics and chemistry* vol 1 (Elsevier)
- [4] Wang B, Anthony S M, Bae S C and Granick S 2009 *Proceedings of the National Academy of Sciences* **106** 15160–15164 (*Preprint* <https://www.pnas.org/doi/pdf/10.1073/pnas.0903554106>) URL <https://www.pnas.org/doi/abs/10.1073/pnas.0903554106>
- [5] Metzler R and Klafter J 2000 *Physics Reports* **339** 1–77 ISSN 0370-1573 URL <https://www.sciencedirect.com/science/article/pii/S0370157300000703>
- [6] Bouchaud J P and Georges A 1990 *Physics Reports* **195** 127–293 ISSN 0370-1573 URL <https://www.sciencedirect.com/science/article/pii/037015739090099N>
- [7] Carr E J and Simpson M J 2019 *The Journal of Chemical Physics* **150** 044104 ISSN 0021-9606 (*Preprint* https://pubs.aip.org/aip/jcp/article-pdf/doi/10.1063/1.5067290/15556183/044104_1_online.pdf) URL <https://doi.org/10.1063/1.5067290>
- [8] Mutohya N M, Xu Y, Li Y and Metzler R 2021 *Journal of Physics A: Mathematical and Theoretical* **54** 295002 URL <https://dx.doi.org/10.1088/1751-8121/abfba6>
- [9] Witzel P, Götz M, Lanoiselée Y, Franosch T, Grebenkov D S and Heinrich D 2019 *Biophysical Journal* **117** 203–213 ISSN 0006-3495 URL <https://www.sciencedirect.com/science/article/pii/S0006349519304965>

- [10] Reister-Gottfried E, Leitenberger S M and Seifert U 2010 *Phys. Rev. E* **81**(3) 031903 URL <https://link.aps.org/doi/10.1103/PhysRevE.81.031903>
- [11] Reister E and Seifert U 2005 *Europhysics Letters* **71** 859 URL <https://dx.doi.org/10.1209/epl/i2005-10139-6>
- [12] Lampo T J, Stylianidou S, Backlund M P, Wiggins P A and Spakowitz A J 2017 *Biophysical Journal* **112** 532–542 ISSN 0006-3495 URL <https://www.sciencedirect.com/science/article/pii/S0006349516343223>
- [13] Toli é Nørrelykke I M, Munteanu E L, Thon G, Oddershede L and Berg-Sørensen K 2004 *Phys. Rev. Lett.* **93**(7) 078102 URL <https://link.aps.org/doi/10.1103/PhysRevLett.93.078102>
- [14] Duan Y, Mahault B, Ma Y q, Shi X q and Chaté H 2021 *Phys. Rev. Lett.* **126**(17) 178001 URL <https://link.aps.org/doi/10.1103/PhysRevLett.126.178001>
- [15] Nattermann T and Vilfan I 1988 *Phys. Rev. Lett.* **61**(2) 223–226 URL <https://link.aps.org/doi/10.1103/PhysRevLett.61.223>
- [16] Cugliandolo L F and Kurchan J 1994 *Journal of Physics A: Mathematical and General* **27** 5749 URL <https://dx.doi.org/10.1088/0305-4470/27/17/011>
- [17] Zhao T, Cao T, Zhan Y and Zhuo Y 2002 *Physica A: Statistical Mechanics and its Applications* **312** 109–118 ISSN 0378-4371 URL <https://www.sciencedirect.com/science/article/pii/S0378437102009603>
- [18] Borile C, Maritan A and Muñoz M A 2013 *Journal of Statistical Mechanics: Theory and Experiment* **2013** P04032 URL <https://dx.doi.org/10.1088/1742-5468/2013/04/P04032>
- [19] Juhász R and Kovács I A 2020 *Phys. Rev. Res.* **2**(1) 013123 URL <https://link.aps.org/doi/10.1103/PhysRevResearch.2.013123>
- [20] Galla T 2024 Generating-functional analysis of random lotka-volterra systems: A step-by-step guide (*Preprint* [2405.14289](https://arxiv.org/abs/2405.14289)) URL <https://arxiv.org/abs/2405.14289>
- [21] Yizhaq H and Bel G 2016 *New Journal of Physics* **18** 023004 URL <https://dx.doi.org/10.1088/1367-2630/18/2/023004>
- [22] Meibohm J and Klapp S H L 2025 *Phys. Rev. Lett.* **134**(8) 087101 URL <https://link.aps.org/doi/10.1103/PhysRevLett.134.087101>
- [23] Tyagi N and Cherayil B J 2017 *The Journal of Physical Chemistry B* **121** 7204–7209 ISSN 1520-6106 URL <https://doi.org/10.1021/acs.jpcb.7b03870>
- [24] Chechkin A V, Seno F, Metzler R and Sokolov I M 2017 *Phys. Rev. X* **7**(2) 021002 URL <https://link.aps.org/doi/10.1103/PhysRevX.7.021002>
- [25] Goswami K and Sebastian K L 2020 *Phys. Rev. E* **102**(4) 042103 URL <https://link.aps.org/doi/10.1103/PhysRevE.102.042103>
- [26] Jain R and Sebastian K L 2017 *Journal of Chemical Sciences* **129** 929–937 ISSN 0973-7103 URL <https://doi.org/10.1007/s12039-017-1308-0>
- [27] Guéneau M, Majumdar S N and Schehr G 2025 Large deviations in switching diffusion: from free cumulants to dynamical transitions (*Preprint* [2501.13754](https://arxiv.org/abs/2501.13754)) URL <https://arxiv.org/abs/2501.13754>
- [28] Santra I, Basu U and Sabhapandit S 2022 *Journal of Physics A: Mathematical and Theoretical* **55** 414002 URL <https://dx.doi.org/10.1088/1751-8121/ac8dcc>
- [29] Khadem S M J, Siboni N H and Klapp S H L 2021 *Phys. Rev. E* **104**(6) 064615 URL <https://link.aps.org/doi/10.1103/PhysRevE.104.064615>
- [30] Zanchetta D, Gupta D, Moschin S, Suweis S, Maritan A and Azaele S 2025 Emergence of ecological structure and species rarity from fluctuating metabolic strategies (*Preprint* [2502.13720](https://arxiv.org/abs/2502.13720)) URL <https://arxiv.org/abs/2502.13720>
- [31] Suweis S, Ferraro F, Grilletta C, Azaele S and Maritan A 2024 *Phys. Rev. Lett.* **133**(16) 167101 URL <https://link.aps.org/doi/10.1103/PhysRevLett.133.167101>
- [32] Ferraro F, Grilletta C, Maritan A, Suweis S and Azaele S 2025 *Journal of Statistical Mechanics: Theory and Experiment* **2025** 023301 URL <https://dx.doi.org/10.1088/1742-5468/adac3f>
- [33] Rozenfeld R, Luczka J and Talkner P 1998 *Physics Letters A* **249** 409–414 ISSN 0375-9601 URL

- <https://www.sciencedirect.com/science/article/pii/S0375960198008238>
- [34] Huang X, Lin L and Wang H 2020 *Journal of Statistical Physics* **178** 1201–1216 ISSN 1572-9613 URL <https://doi.org/10.1007/s10955-020-02494-3>
 - [35] Gitterman M et al. 2012 *World Journal of Mechanics* **2** 113
 - [36] Burov S and Gitterman M 2016 *Phys. Rev. E* **94**(5) 052144 URL <https://link.aps.org/doi/10.1103/PhysRevE.94.052144>
 - [37] Alston H, Cocconi L and Bertrand T 2022 *Journal of Physics A: Mathematical and Theoretical* **55** 274004 URL <https://dx.doi.org/10.1088/1751-8121/ac726b>
 - [38] Gomez-Solano J R, Bellon L, Petrosyan A and Ciliberto S 2010 *Europhysics Letters* **89** 60003 URL <https://dx.doi.org/10.1209/0295-5075/89/60003>
 - [39] Pal A and Sabhapandit S 2013 *Phys. Rev. E* **87**(2) 022138 URL <https://link.aps.org/doi/10.1103/PhysRevE.87.022138>
 - [40] Hänggi P and Bartschek R 1996 *Nonlinear Physics of Complex Systems: Current Status and Future Trends* **476** 294 – 308
 - [41] Doering C R 1998 *Physica A: Statistical Mechanics and its Applications* **254** 1–6 ISSN 0378-4371 URL <https://www.sciencedirect.com/science/article/pii/S0378437198000065>
 - [42] Venturelli D, Loos S A M, Walter B, Roldan E and Gambassi A 2024 *Europhysics Letters* **146** 27001 URL <https://dx.doi.org/10.1209/0295-5075/ad3469>
 - [43] Gupta D, Pal A and Kundu A 2021 *Journal of Statistical Mechanics: Theory and Experiment* **2021** 043202 URL <https://dx.doi.org/10.1088/1742-5468/abefdf>
 - [44] Gupta D, Plata C A, Kundu A and Pal A 2020 *Journal of Physics A: Mathematical and Theoretical* **54** 025003 URL <https://dx.doi.org/10.1088/1751-8121/abcf0b>
 - [45] Goerlich R, Li M, Pires L B, Hervieux P A, Manfredi G and Genet C 2024 Taming a maxwell’s demon for experimental stochastic resetting (*Preprint* 2306.09503) URL <https://arxiv.org/abs/2306.09503>
 - [46] Besga B, Bovon A, Petrosyan A, Majumdar S N and Ciliberto S 2020 *Phys. Rev. Res.* **2**(3) 032029 URL <https://link.aps.org/doi/10.1103/PhysRevResearch.2.032029>
 - [47] Olsen K S, Gupta D, Mori F and Krishnamurthy S 2024 *Physical Review Research* **6** 033343
 - [48] Gupta D and Plata C A 2022 *New Journal of Physics* **24** 113034
 - [49] Olsen K S and Gupta D 2024 *Journal of Physics A: Mathematical and Theoretical* **57** 245001
 - [50] Gupta D, Olsen K S and Krishnamurthy S 2025 Thermodynamic cost of recurrent erasure (*Preprint* 2502.06014) URL <https://arxiv.org/abs/2502.06014>
 - [51] Mercado-Vásquez G, Boyer D, Majumdar S N and Schehr G 2020 *Journal of Statistical Mechanics: Theory and Experiment* **2020** 113203 URL <https://dx.doi.org/10.1088/1742-5468/abc1d9>
 - [52] Santra I, Das S and Nath S K 2021 *Journal of Physics A: Mathematical and Theoretical* **54** 334001 URL <https://dx.doi.org/10.1088/1751-8121/ac12a0>
 - [53] Biroli M, Kulkarni M, Majumdar S N and Schehr G 2024 *Phys. Rev. E* **109**(3) L032106 URL <https://link.aps.org/doi/10.1103/PhysRevE.109.L032106>
 - [54] Lu X J, Muga J G, Chen X, Poschinger U G, Schmidt-Kaler F and Ruschhaupt A 2014 *Phys. Rev. A* **89**(6) 063414 URL <https://link.aps.org/doi/10.1103/PhysRevA.89.063414>
 - [55] Lu X J, Ruschhaupt A and Muga J G 2018 *Phys. Rev. A* **97**(5) 053402 URL <https://link.aps.org/doi/10.1103/PhysRevA.97.053402>
 - [56] Meinhold L, Smith J C, Kitao A and Zewail A H 2007 *Proceedings of the National Academy of Sciences* **104** 17261–17265 (*Preprint* <https://www.pnas.org/doi/pdf/10.1073/pnas.0708199104>) URL <https://www.pnas.org/doi/abs/10.1073/pnas.0708199104>
 - [57] Shtelen W M and Stogny V I 1989 *Journal of Physics A: Mathematical and General* **22** L539 URL <https://dx.doi.org/10.1088/0305-4470/22/13/002>
 - [58] Suzuki M 1985 *Journal of Mathematical Physics* **26** 601–612 ISSN 0022-2488 (*Preprint* https://pubs.aip.org/aip/jmp/article-pdf/26/4/601/19120226/601_1_online.pdf) URL <https://doi.org/10.1063/1.526596>
 - [59] Cocconi L, Alston H, Romano J and Bertrand T 2024 *New Journal of Physics* **26** 103016 URL

- <https://dx.doi.org/10.1088/1367-2630/ad7ef1>
- [60] Touchette H 2009 Physics Reports **478** 1–69 ISSN 0370-1573 URL <https://www.sciencedirect.com/science/article/pii/S0370157309001410>
- [61] Sekimoto K 2010 Stochastic energetics
- [62] Gupta D and Sivak D A 2021 Phys. Rev. E **104**(2) 024605 URL <https://link.aps.org/doi/10.1103/PhysRevE.104.024605>
- [63] Kundu A, Sabhapandit S and Dhar A 2011 Journal of Statistical Mechanics: Theory and Experiment **2011** P03007 URL <https://dx.doi.org/10.1088/1742-5468/2011/03/P03007>
- [64] Goerlich R, Li M, Pires L B, Hervieux P A, Manfredi G and Genet C 2023 arXiv preprint arXiv:2306.09503
- [65] Risken H 1989 Fokker-planck equation The Fokker-Planck equation: methods of solution and applications (Springer) pp 63–95